© 2019. Published by The Company of Biologists Ltd | Biology Open (2019) 8, bio047126. doi:10.1242/bio.047126

RESEARCH ARTICLE

Heparan sulfate negatively regulates intestinal stem cell proliferation in *Drosophila* adult midgut

Hubing Ma*, Huiqing Zhao*, Fuli Liu*, Hang Zhao, Ruiyan Kong, Lin Shi, Min Wei and Zhouhua Li‡

ABSTRACT

Tissue homeostasis is maintained by differentiated progeny of residential stem cells. Both extrinsic signals and intrinsic factors play critical roles in the proliferation and differentiation of adult intestinal stem cells (ISCs). However, how extrinsic signals are transduced into ISCs still remains unclear. Here, we find that heparan sulfate (HS), a class of glycosaminoglycan (GAG) chains, negatively regulates progenitor proliferation and differentiation to maintain midgut homeostasis under physiological conditions. Interestingly, HS depletion in progenitors results in inactivation of Decapentaplegic (Dpp) signaling. Dpp signal inactivation in progenitors resembles *HS-deficient* intestines. Ectopic Dpp signaling completely rescued the defects caused by HS depletion. Taken together, these data demonstrate that HS is required for Dpp signaling to maintain midgut homeostasis. Our results provide insight into the regulatory mechanisms of how extrinsic signals are transduced into stem cells to regulate their proliferation and differentiation.

KEY WORDS: Intestinal stem cell, Heparan sulfate, *Drosophila*, Tissue homeostasis, Dpp signaling

INTRODUCTION

Adult stem cells are responsible for tissue homeostasis in the tissues in which they reside; frequently lost cells are constantly replenished by the progeny of stem cells. The proliferation and differentiation of adult stem cells must be tightly balanced. Disruption of this balance will lead to either excessive stem cells or stem cell depletion, eventually resulting in various diseases, such as cancer (Lin, 2008; Morrison and Spradling, 2008; Radtke and Clevers, 2005; Xie and Spradling, 1998). Therefore, understanding of the underlying mechanisms controlling adult stem cell proliferation and differentiation will provide insight into the potential development of therapeutic applications for human diseases.

The posterior midgut of the adult *Drosophila* intestine is an excellent system to study how stem cell proliferation and differentiation are regulated. Mammalian and *Drosophila* intestines show marked similarities in terms of development, cellular make-up and genetic control (Casali and Batlle, 2009; Edgar, 2012; Stainier, 2005; Wang and Hou, 2010). Adult intestinal stem cells (ISCs) are interspersed along the base membrane of the *Drosophila* adult midgut (Micchelli and Perrimon, 2006; Ohlstein and Spradling, 2006). Initial studies proposed that ISCs constantly undergo asymmetric divisions and produce non-dividing enteroblasts (EBs) (Micchelli and Perrimon, 2006; Ohlstein and Spradling, 2006). The ligand of the Notch pathway, Delta (Dl), is specifically expressed in ISCs, while Notch receptor is expressed in both ISCs and EBs. ISCs signal via Dl to activate Notch signaling in EBs (Ohlstein and Spradling, 2007). EBs terminally differentiate into either an absorptive enterocyte (EC) or a secretory enteroendocrine cell (ee) depending on their signaling environments (Beebe et al., 2010; Micchelli and Perrimon, 2006; Ohlstein and Spradling, 2007; Perdigoto et al., 2011; Yeung et al., 2011). Recent studies demonstrate that in response to differentiation and subsequent loss of a neighboring ISC (or vice versa), a significant proportion of ISCs divide symmetrically (de Navascués et al., 2012; Goulas et al., 2012; O'Brien et al., 2011). Moreover, ee cells may not be generated from EBs, but directly from ISCs or ee progenitor cells (EEPs) (Biteau and Jasper, 2014; Chen et al., 2018; Zeng et al., 2015). Interestingly, unlike in other systems in which differentiated cells can de-differentiate into stem cells, we found that no regeneration of new ISCs could be observed after all the progenitors were ablated in the intestines, indicating that fully differentiated cells are likely unable to de-differentiate into ISCs when all the progenitors are depleted (Brawley and Matunis, 2004; Lu and Li, 2015; Raff, 2003).

Numerous studies have shown that ISC proliferation and differentiation under physiological conditions and during tissue regeneration are regulated by many signaling pathways and intrinsic factors, including the Notch, Wingless (Wg), Janus Kinase/Signal Transducer and Activator of Transcription (JAK/STAT), Epidermal Growth Factor Receptor (EGFR), Hippo (Hpo), Insulin, Hedgehog (Hh) and Bone Morphogenetic Protein (BMP) signaling pathways (Amcheslavsky et al., 2009; Biteau and Jasper, 2011; Buchon et al., 2009; Chakrabarti et al., 2016; Chen et al., 2016; Choi et al., 2011; Cordero et al., 2012; Guo and Ohlstein, 2015; Han et al., 2015; Jiang et al., 2011, 2009; Jin et al., 2017; Karpowicz et al., 2010; Lee et al., 2009; Li et al., 2013a,b, 2014; Lin and Xi, 2008; Lin et al., 2008; Martorell et al., 2014; Ohlstein and Spradling, 2006, 2007; Rahman et al., 2017; Ren et al., 2010, 2015; Schell et al., 2017; Shaw et al., 2010; Singh et al., 2016; Staley and Irvine, 2010; Tian and Jiang, 2014; Tian et al., 2015, 2017; Xu et al., 2011; Zhai et al., 2017; Zhou et al., 2015). However, it remains unclear how extrinsic signals are transduced into ISCs to regulate their proliferation and differentiation under physiological conditions.

Heparan sulfate chains are attached to the core protein of heperan sulfate proteoglycans (HSPGs), macromolecules presented on the cell surface and in the extracellular matrix (ECM). There are three evolutionarily conserved families of HSPGs: Glypicans and Syndecans are two major cell surface HSPGs, while Perlecans are secreted HSPGs that are mainly distributed in the ECM (Esko and Lindahl, 2001; Esko and Selleck, 2002; Lin, 2004). HS chain biosynthesis is initiated in the Golgi apparatus at the GAG

College of Life Sciences, Capital Normal University, Beijing 100048, China.
*These authors contributed equally to this work

‡Author for correspondence (zhli@cnu.edu.cn)

Z.L., 0000-0002-7660-8579

Received 20 August 2019; Accepted 30 September 2019

Biology Open (2019) 8, bio047126. doi:10.1242/bio.047126

attachment site(s) of the core protein. HS is synthesized by a series of conserved HS biosynthetic and modifying enzymes, including Gal transferases, the exostosin (EXT) proteins [Tout-velu (Ttv), Sister of ttv (Sotv), Brother of ttv (Botv)], Sulfateless (Sfl) and Sugarless (Sgl) (Esko and Lindahl, 2001; Esko and Selleck, 2002; Lin, 2004). Previous studies demonstrate that HSPGs are required for the distribution of several well-known morphogens, including Wg, Hh, Upd and Dpp (Belenkaya et al., 2004; Bellaiche et al., 1998; Binari et al., 1997; Bornemann et al., 2004; Dani et al., 2012; Filmus et al., 2008; Fujise et al., 2003; Jackson et al., 1997; Kamimura et al., 2006; Levings and Nakato, 2017; Lin and Perrimon, 1999, 2000, 2002; Liu et al., 2010; Mii et al., 2017; Takei et al., 2004; Yan and Lin, 2009; Yu et al., 2017; Zhang et al., 2013). Although HS plays important roles in the functions of HSPGs, its role(s) in regulating ISC proliferation and differentiation under physiological conditions remains elusive.

In this study, we provide evidence that HS in progenitors restricts ISC proliferation and differentiation under normal homeostasis. Importantly, we demonstrate that HS is required for Dpp signal activation. Thus, our data uncover a mechanism of HS to maintain midgut homeostasis.

RESULTS

Loss of HS in progenitors leads to disruption of midgut homeostasis

In order to identify intrinsic factors regulating the proliferation and differentiation of ISCs, we carried out a genome-wide RNAi screen using the *esgGal4, UAS-GFP, tubGal80^{ts}* (*esg^{ts}*) driver in the posterior midgut. *esgGal4* is expressed in progenitors (ISCs and EBs) in the midgut. 11,316 RNAi lines from Vienna *Drosophila* RNAi Center (VDRC), Fly stocks of National Institute of Genetics (NIG-FLY), and the Transgenic RNAi Project (TRiP) at Harvard Medical School/Tsinghua University were screened (manuscript in preparation). Many factors affecting ISC maintenance, viability and proliferation/differentiation were identified from this screen. Among these factors, HS biosynthetic enzymes (including Sfl, Sgl and the EXT proteins) were identified as candidates. Only single or paired *esg*$^+$ cells are observed in control flies (Fig. 1A). However, the number of *esg*$^+$ cells was significantly increased when *sfl* was depleted in progenitors. *esg*$^+$ cells formed clusters and GFP was expressed in polyploid cells, indicative of midgut homeostasis loss (Fig. 1B,C,I). *sfl* encodes the only *Drosophila* HS N-deacetylase/N-sulfotransferase, which catalyzes the first step of HS modification (Esko and Lindahl, 2001; Lin, 2004). The RNAi off-target effect could be excluded as induction of two independent RNAi constructs against *sfl* produced a similar phenotype (Fig. 1B,C,I) and the knockdown efficacy of these RNAi lines was confirmed by qRT-PCR (Fig. S1). When *sgl* and EXT genes were knocked down, midgut homeostasis was also lost (Fig. 1D,I). Consistent with the increase of progenitors, we observed a significant increase of the number of cells undergoing mitosis in these intestines (Fig. 1J; Fig. S2). Meanwhile, many large *esg*$^+$ cells expressed mature EC-marker PDM1, indicative of intestinal homeostasis loss (Fig. S3). Previous studies had demonstrated that mutations in these HS biosynthetic genes led to striking reductions in HS levels (Bornemann et al., 2004; Han et al., 2004; Takei et al., 2004; Toyoda et al., 2000a,b). Consistently, we found HS was effectively abrogated in *tub^{ts}>botv^{RNAi}* intestines (Fig. S4). These data demonstrate that HS in progenitors restricts ISC proliferation, thereby maintaining midgut homeostasis. As EXT3/Botv participates in the earliest steps of HS biosynthesis, we mainly focused on *botv* for further analysis.

HS in progenitors negatively regulates ISC proliferation and differentiation

We examined the identity of these *esg*$^+$ cells in the absence of HS. We found that the number of ISCs (by Dl and *Dl-lacZ*) in *esg^{ts}>sfl^{RNAi}* and *esg^{ts}>botv^{RNAi}* intestines was significantly increased compared to those in the control flies (Fig. 2A–C,E–F). The number of EBs [by *GBE+Su(H)-lacZ*] was also significantly increased in *esg^{ts}>botv^{RNAi}* intestines compared to those in the control flies (Fig. 2H–J). However, no obvious change in the number of ee cells (by Pros) was observed in these intestines (Fig. 2A–D). We found that the size of the large GFP$^+$ cells (premature/mature ECs) was smaller than that of fully differentiated ECs, indicating that HS may also regulate EC maturation (Fig. 2H,I). We also observed a significant increase of ISCs when HS synthesis was disrupted in ISCs using ISC-specific driver *Dl^{ts}* (data not shown). Taken together, these data demonstrate that HS in progenitors negatively regulates ISC proliferation and differentiation under physiological conditions.

Consistent with increased ISC proliferation, we found the number of *10xSTATGFP*$^+$ cells and the intensity of *10xSTATGFP* signal in *esg^{ts}>botv^{RNAi}* intestines were both significantly increased compared to those in the control flies (Fig. S5A–D). However, the expression of the JAK/STAT pathway cytokines (*Upd1-3*) was only mildly increased in *esg^{ts}>botv^{RNAi}* intestines compared to those in control intestines as determined by qRT-PCR (Fig. S6A). We examined whether the accumulation of *esg*$^+$ cells observed in *esg^{ts}>botv^{RNAi}* intestines resulted from the expression of cytokines in progenitors. We found that neither individual nor simultaneous depletion of cytokines could suppress the accumulation of *esg*$^+$ cells observed in those intestines (Fig. S6B–L). These data indicate that cytokines are unlikely produced in these *HS-deficient* progenitors.

HSPGs (except Perlecan) may play redundant roles in progenitor proliferation

HSPGs comprise a core protein to which HS chains are attached. Our data demonstrate that HS in progenitors inhibits ISC proliferation. We explored which HSPG(s) are required for ISC proliferation. A previous study indicated that loss of the core protein of Perlecan (Per) caused detachment of ISC from basement membrane, resulting in loss of ISC proliferation (You et al., 2014). Dally and Dally-like (Dlp) are two major Glypicans in *Drosophila* (Esko and Lindahl, 2001; Esko and Selleck, 2002; Lin, 2004). We examined whether the other HSPGs, except Per, are required for ISC proliferation. We first examined the expression pattern of Dally and Dlp in the intestines. We found that Dally was mainly expressed in ECs (Fig. S7A,B), while Dlp was mainly expressed in the visceral muscles (VMs), and at low levels in the midgut epithelium (Fig. S7C,D). Effective RNAi constructs against *dally* and *dlp* were utilized to explore whether these HSPGs are required for ISC proliferation (Zhang et al., 2013). We found that neither individual nor combinational knockdown of *dally* and *dlp* affected ISC proliferation significantly (Fig. S7E–H). We also found that neither individual nor combinational knockdown of the other HSPGs, *sdc* and *cow*, as significantly affected ISC proliferation as those observed in HS-deficient progenitors (data not shown). These data indicate that these HSPGs (except Per) may play redundant roles in ISC proliferation. Therefore, we focused on HS chains, but not individual HSPGs, for further investigation.

HS is required for Dpp signal activation in progenitors

The above mentioned experiments demonstrate that HS in progenitors is required for midgut homeostasis under normal conditions. We explored the underlying mechanism of how HS

Biology Open (2019) 8, bio047126. doi:10.1242/bio.047126

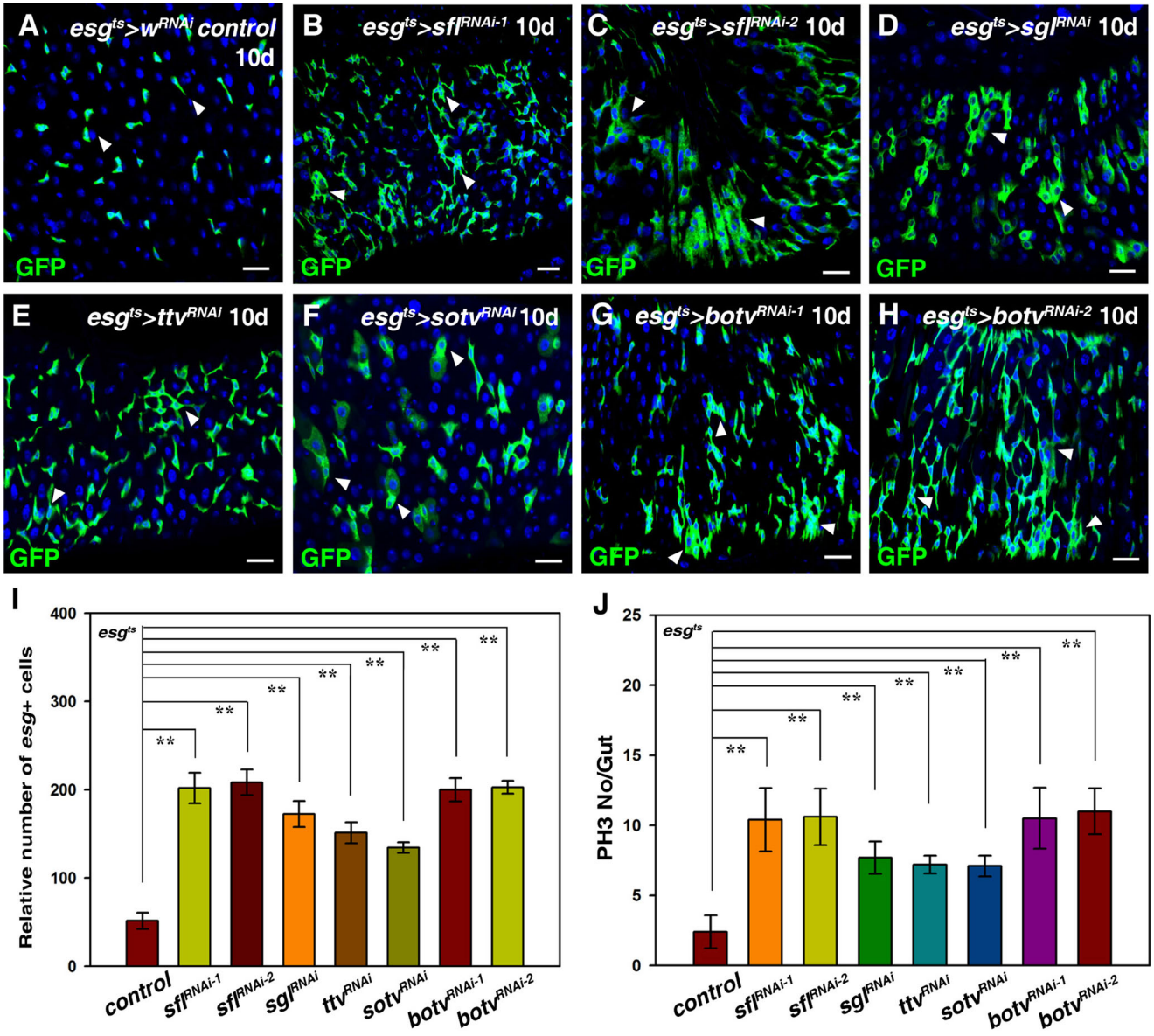

Fig. 1. HS in progenitors restricts ISC proliferation. (A) *esg*$^+$ cells (green) in control flies at 29°C for 10 days (white arrowheads). (B,C) The number of *esg*$^+$ cells (green) is dramatically increased in *esg*^{ts}*>sfl*^{RNAi} flies at 29°C for 10 days (white arrowheads). (D) The number of *esg*$^+$ cells (green) is dramatically increased in *esg*^{ts}*>sgl*^{RNAi} flies at 29°C for 10 days (white arrowheads). (E) The number of *esg*$^+$ cells (green) is dramatically increased in *esg*^{ts}*>ttv*^{RNAi} flies at 29°C for 10 days (white arrowheads). (F) The number of *esg*$^+$ cells (green) is dramatically increased in *esg*^{ts}*>sotv*^{RNAi} flies at 29°C for 10 days (white arrowheads). (G,H) The number of *esg*$^+$ cells (green) is dramatically increased in *esg*^{ts}*>botv*^{RNAi} flies at 29°C for 10 days (white arrowheads). (I) Quantification of the relative number of *esg*$^+$ cells in the different genotypes indicated. mean±s.d. is shown. *n*=10–15 intestines. ***P*<0.01. (J) Quantification of the number of pH3 per gut in the different genotypes indicated. mean±s.d. is shown. *n*=10–15 intestines. ***P*<0.01. In all panels except graphs, GFP is in green and blue indicates DAPI staining for DNA. Scale bars: 20 µm.

controls midgut homeostasis. HS is required for the activation of many signaling pathways, including Wg, JAK/STAT, Notch and BMP (Belenkaya et al., 2004; Bellaiche et al., 1998; Binari et al., 1997; Bornemann et al., 2004; Dani et al., 2012; Filmus et al., 2008; Fujise et al., 2003; Jackson et al., 1997; Kamimura et al., 2006; Levings and Nakato, 2017; Lin and Perrimon, 1999, 2000, 2002; Liu et al., 2010; Mii et al., 2017; Takei et al., 2004; Yan and Lin, 2009; Yu et al., 2017; Zhang et al., 2013). Interestingly, the majority of these signaling pathways positively regulate ISC proliferation and differentiation, while Dpp signaling negatively regulates ISC proliferation and differentiation (Guo et al., 2013; Jiang and Edgar, 2009; Jiang et al., 2011, 2009; Li et al., 2013a,b, 2014; Lin et al., 2008; Tian and Jiang, 2014; Tian et al., 2015; Zhou et al., 2015). Notch signaling is not blocked upon loss of HS as the number of *GBE+Su(H)-lacZ*$^+$ cells was dramatically increased, indicating that Notch signaling is not affected by HS depletion (Fig. 2H–J). Therefore, we speculated that HS may be required for Dpp signal activation in progenitors. To confirm our hypothesis, we examined Dpp signal activation in the absence of HS. Dpp signaling (by pMAD) is mainly activated in ECs, but also in progenitors in control flies (Fig. 3A) (Li et al., 2013b; Tian and Jiang, 2014; Zhou et al., 2015). When HS was depleted in progenitors, pMAD signal in progenitors was abolished, supporting the notion that HS is required for Dpp signal activation in progenitors (Fig. 3A–C).

Biology Open (2019) 8, bio047126. doi:10.1242/bio.047126

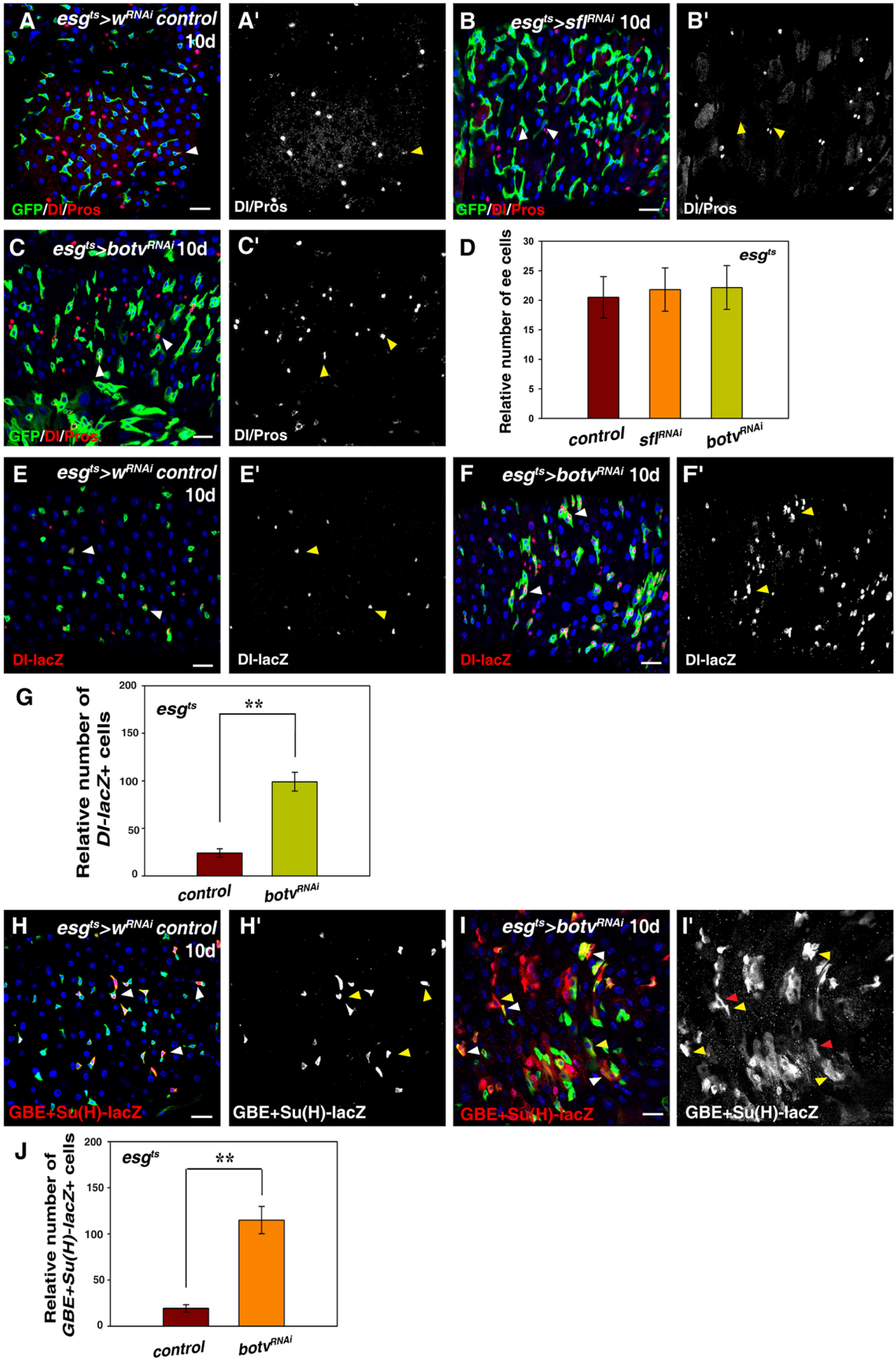

Fig. 2. See next page for legend.

Biology Open

Biology Open (2019) 8, bio047126. doi:10.1242/bio.047126

Fig. 2. HS in progenitors negatively regulates ISC proliferation and differentiation. (A) Dl (ISC marker) and Pros (ee marker) (red) in control intestines (white arrowhead). Split channel for Dl and Pros (A′, in grayscale) in control intestines (yellow arrowhead). (B) Dl and Pros (red) in esg^{ts}>sfl^{RNAi} intestines (white arrowheads). Split channel for Dl and Pros (B′, in grayscale) in esg^{ts}>sfl^{RNAi} intestines (yellow arrowheads). (C) Dl and Pros (red) in esg^{ts}>$botv^{RNAi}$ intestines (white arrowheads). Split channel for Dl and Pros (C′, in grayscale) in esg^{ts}>$botv^{RNAi}$ intestines (yellow arrowheads). (D) Quantification of the relative number of ee cells in intestines with indicated phenotypes. *n*=10–15 intestines. mean±s.d. is shown. No obvious change in the number of ee cells is observed. (E) *Dl-lacZ* (red) in control intestines (white arrowheads). Split channel for *Dl-lacZ* (E′, in grayscale) in control intestines (yellow arrowheads). (F) *Dl-lacZ* (red) in esg^{ts}>$botv^{RNAi}$ intestines (white arrowheads). Split channel for *Dl-lacZ* (F′, in grayscale) in esg^{ts}>$botv^{RNAi}$ intestines (yellow arrowheads). (G) Quantification of the relative number of *Dl-lacZ*$^{+}$ cells in control and esg^{ts}>$botv^{RNAi}$ intestines. *n*=10–15 intestines. mean±s.d. is shown. ***P*<0.01. (H) EBs [by *GBE+Su(H)-lacZ* in red] in control intestines (white arrowheads). Split channel for *GBE+Su(H)-lacZ* (H′, in grayscale) in control intestines (yellow arrowheads). (I) The number of EBs [by *GBE+Su(H)-lacZ* in red] is dramatically increased in esg^{ts}>$botv^{RNAi}$ intestines (white and yellow arrowheads). Split channel for *GBE+Su(H)-lacZ* (I′, in grayscale) in esg^{ts}>$botv^{RNAi}$ intestines (yellow and red arrowheads). Note that the size of the larger *GBE+Su(H)-lacZ*$^{+}$ cells is smaller compared to the size of the neighboring wild-type EC cells [polyploid *GBE+Su(H)-lacZ*$^{-}$ cells], indicating that HS chains also affect EC maturation (yellow arrowheads in I). (J) Quantification of the relative number of *GBE+Su(H)-lacZ*$^{+}$ cells in control and esg^{ts}>$botv^{RNAi}$ intestines. *n*=10–15 intestines. mean±s.d. is shown. ***P*<0.01. GFP in green, blue indicates DAPI staining for DNA. Scale bars: 20 µm.

Dpp signaling negatively regulates ISC proliferation and midgut homeostasis under physiological conditions

We then explored whether the defects observed in HS-depletion intestines are direct consequences of Dpp signal inactivation. We first depleted the expression of several key components of the Dpp signaling pathway, including the type II receptor Punt (Put), the type I receptor Thickveins (Tkv) and Mother against Dpp (Mad), in the progenitors using functional RNAi constructs by the esg^{ts} driver (Li et al., 2013b; Xu et al., 2018). We found that the number of esg^{+} cells was dramatically increased in these intestines and many polyploid cells expressed GFP, indicative of midgut homeostasis loss (Fig. 4A–D,F). The observed phenotypes are almost identical to those of HS depletion. We further ectopically expressed *brinker* (*brk*) in progenitors to block Dpp signaling (Jaźwińska et al., 1999). Similarly, the number of esg^{+} cells was dramatically increased in esg^{ts}>*brk* intestines, and esg^{+} cells formed clusters with many polyploid cells expressing GFP (Fig. 4E,F). Consistently, we observed a significant increase of the number of $pH3^{+}$ cells in these intestines (Fig. 4F; Fig. S8). These data show that Dpp signaling negatively regulates ISC proliferation and midgut homeostasis under physiological conditions.

We examined the identity of the esg^{+} cells upon Dpp signaling inactivation in progenitors. We found that the number of ISCs (by Dl and *Dl-lacZ*) in esg^{ts}>tkv^{RNAi} intestines was significantly increased compared to those in the control flies (Fig. S9A,B, and data not shown). No obvious change in the number of ee cells was observed in these intestines (Fig. S9A,B). We found the number of EBs [by *GBE+Su(H)-lacZ*] was also significantly increased in esg^{ts}>put^{RNAi} and esg^{ts}>tkv^{RNAi} intestines compared to those in the control flies (Fig. S9C–F). Consistently, we found that the size of the polyploid GFP^{+} cells was smaller than fully differentiated ECs, indicating that Dpp signaling may also regulate EC maturation (Fig. S9C–E). Furthermore, we generated *tkv* ISC clones using the MARCM technique (Lee and Luo, 2001). We utilized two amorphic *tkv* mutants, tkv^{8} and tkv^{a12}. The ISC clone size of both *tkv* mutants was significantly increased compared with control clones (Fig. 4H–K). Together, these data demonstrate that Dpp signaling in progenitors

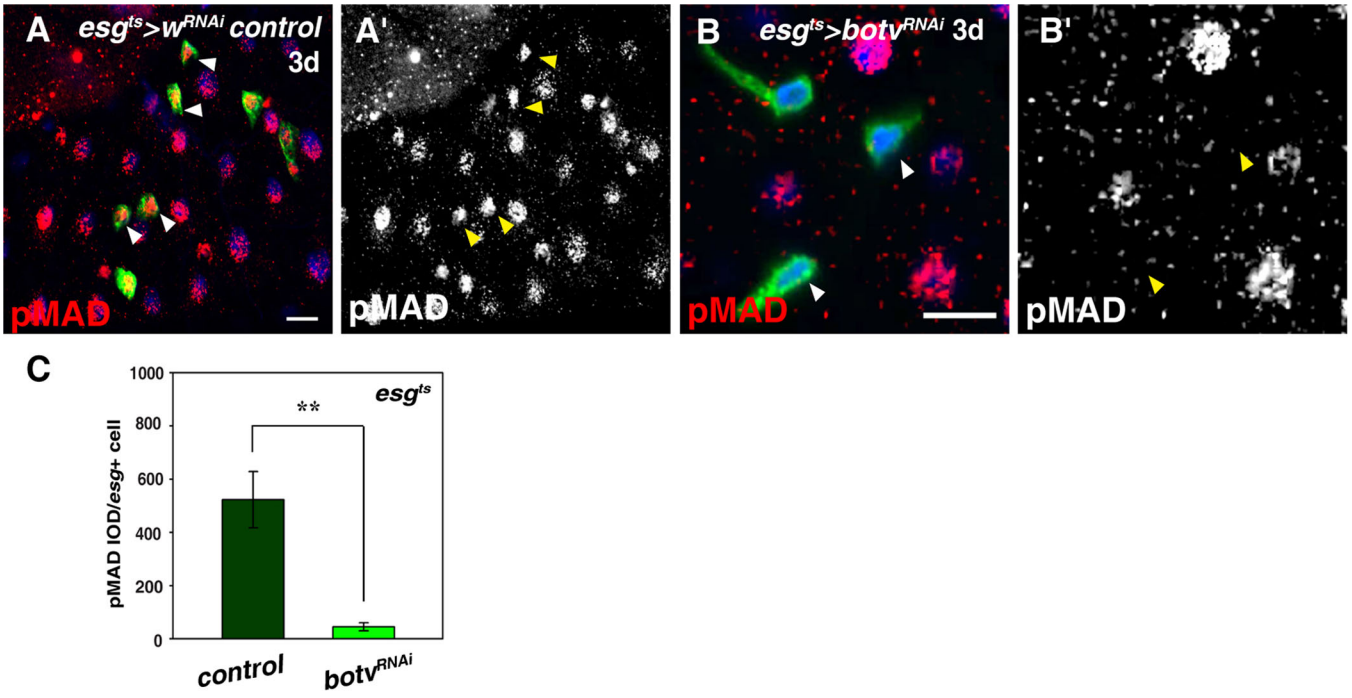

Fig. 3. Loss of HS leads to Dpp signal inactivation. (A) Dpp signaling (by pMAD in red) in control intestines. Dpp signaling is highly activated in ECs and progenitors (green) (white arrowheads). Split channel for pMAD (A′, in grayscale) (yellow arrowheads). (B) Dpp signaling (by pMAD in red) in progenitors is eliminated in esg^{ts}>$botv^{RNAi}$ intestines (white arrowheads). Split channel for pMAD (B′, in grayscale) (yellow arrowheads). (C) Quantification of by pMAD signal after knockdown of *botv* in progenitors. IOD was used. *n*≥4. mean±s.d. is shown. ***P*<0.01. In all panels except graphs, GFP is in green, blue indicates DAPI staining for DNA. Scale bars: 20 µm.

Biology Open (2019) 8, bio047126. doi:10.1242/bio.047126

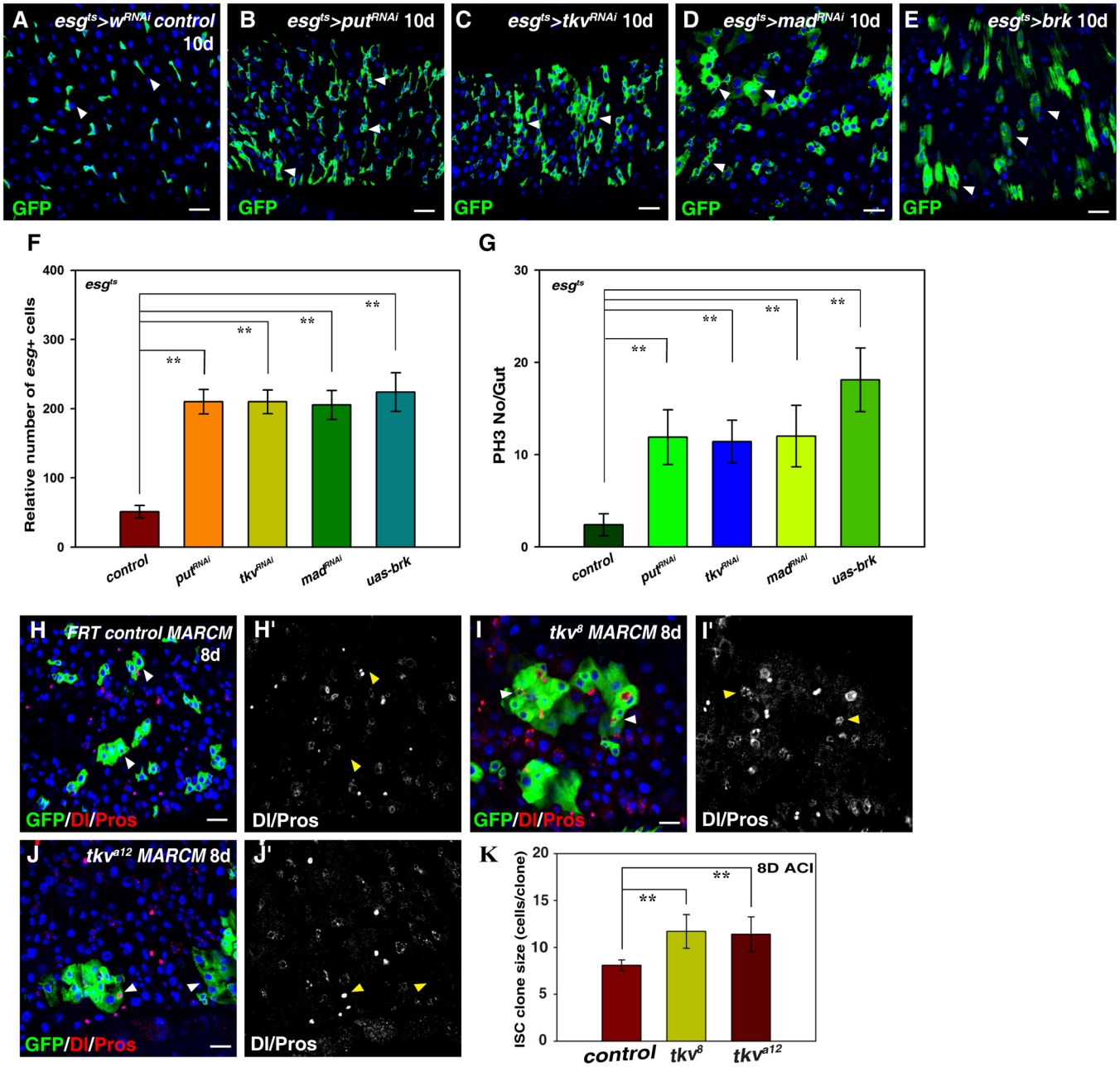

Fig. 4. Dpp signaling in ISCs restricts ISC proliferation. (A) *esg*$^{+}$ cells (green) in control flies at 29°C for 10 days (white arrowheads). (B) The number of *esg*$^{+}$ cells (green) is dramatically increased in *esg*^{ts}>*put*^{RNAi} flies at 29°C for 10 days (white arrowheads). (C) The number of *esg*$^{+}$ cells (green) is dramatically increased in *esg*^{ts}>*tkv*^{RNAi} flies at 29°C for 10 days (white arrowheads). (D) The number of *esg*$^{+}$ cells (green) is dramatically increased in *esg*^{ts}>*mad*^{RNAi} flies at 29°C for 10 days (white arrowheads). (E) The number of *esg*$^{+}$ cells (green) is dramatically increased in *esg*^{ts}>*brk* flies at 29°C for 10 days (white arrowheads). (F) Quantification of the relative number of *esg*$^{+}$ cells in different genotypes indicated. mean±s.d. is shown. *n*=10–15 intestines. ***P*<0.01. (G) Quantification of the number of pH3/gut in different genotypes indicated. mean±s.d. is shown. *n*=10–15 intestines. ***P*<0.01. (H) ISC MARCM clones (green) in *FRT* control (8 days at 25°C, 8D ACI) (white arrowheads). Dl and Pros in red. Split channel for Dl and Pros (H′, in grayscale) (yellow arrowheads). (I,J) The size of *tkv*^{8} (I) and *tkv*^{a12} (J) ISC MARCM clones (green) is significantly increased (8D ACI) (white arrowheads). Dl and Pros in red. Split channel for Dl and Pros (I′,J′, in grayscale) (yellow arrowheads). (K) Quantification of ISC clone size in control and *tkv* mutants (8D ACI). Note that the size of *tkv* mutant ECs is smaller than neighboring wild-type ECs. mean±s.d. is shown. *n*=10. ***P*<0.01. In all panels except graphs, GFP is in green, blue indicates DAPI staining for DNA. Scale bars: 20 µm. Note that images for the control flies in A are reproduced from Fig. 1.

negatively regulates ISC proliferation and differentiation to maintain midgut homeostasis under normal conditions.

To further confirm that Dpp signaling inactivation is the direct consequence of HS disruption, we performed rescue experiments. Our rationale is: if Dpp signal inactivation is the direct consequence of HS disruption, then restoring Dpp signaling in *HS-depleted* intestines will completely rescue the defects observed in *HS-deficient* intestines. Interestingly, co-expression of a constitutively active form of *tkv* (*tkv*^{CA}) with either *sfl*^{RNAi} or *botv*^{RNAi} completely rescued the defects observed in *esg*^{ts}>*sfl*^{RNAi} and *esg*^{ts}>*botv*^{RNAi} intestines respectively (Fig. 5A–G). Moreover, the increased number of ISCs undergoing mitosis was also completely rescued in these

Biology Open (2019) 8, bio047126. doi:10.1242/bio.047126

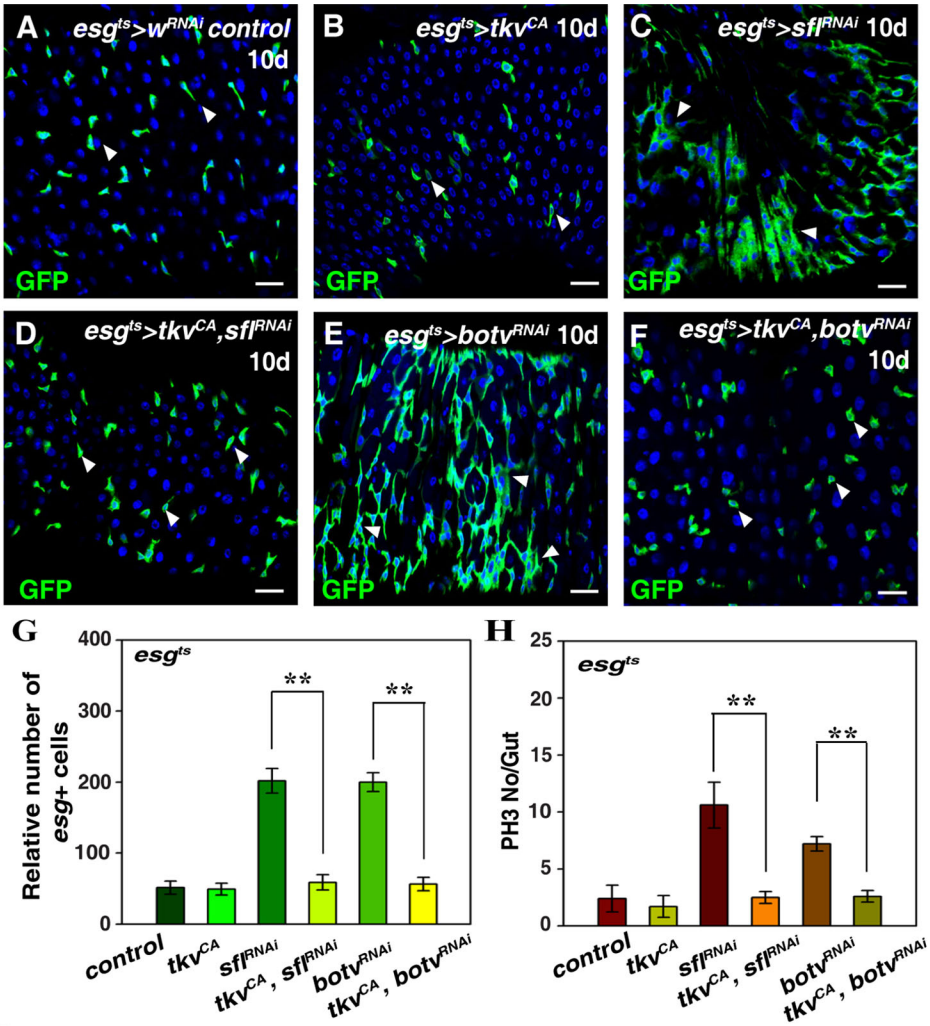

Fig. 5. Ectopic activation of Dpp signaling completely rescued defects observed in the absence of HS. (A) *esg*$^{+}$ cells (green) in control flies at 29°C for 10 days (white arrowheads). (B) Progenitors (ISC+EBs, green) in *esg*^{ts}>*tkv*^{CA} intestines (white arrowheads). (C) The number of *esg*$^{+}$ cells (green) is dramatically increased in *esg*^{ts}>*sfl*^{RNAi} flies at 29°C for 10 days (white arrowheads). (D) Expression of *tkv*^{CA} could completely rescue increased ISC proliferation observed in *esg*^{ts}>*sfl*^{RNAi} intestines (white arrowheads). (E) The number of *esg*$^{+}$ cells (green) is dramatically increased in *esg*^{ts}>*botv*^{RNAi} flies at 29°C for 10 days (white arrowheads). (F) Expression of *tkv*^{CA} could completely rescue increased ISC proliferation observed in *esg*^{ts}>*botv*^{RNAi} intestines (white arrowheads). (G) Quantification of the relative number of *esg*$^{+}$ cells in different genotypes indicated. mean ±s.d. is shown. *n*=10–15 intestines. $^{**}P<0.01$. (H) Quantification of the number of pH3 per gut in different genotypes indicated. mean±s.d. is shown. *n*=10–15 intestines. $^{**}P<0.01$. (I) Model of HS function in progenitor cells. In all panels except graphs, GFP is in green, blue indicates DAPI staining for DNA. Scale bars: 20 µm. Note that images for the control flies in A,C and E are reproduced from Fig. 1.

Biology Open (2019) 8, bio047126. doi:10.1242/bio.047126

intestines (Fig. 5H; Fig. S10). These data indicate that Dpp signal inactivation is very likely the direct consequence of HS depletion. Taken together, these data show that HS is required for Dpp signaling in progenitors to maintain midgut homeostasis under physiological conditions (Fig. 5I).

DISCUSSION

Residential stem cells must respond to extrinsic signals to properly adjust their proliferation and differentiation rate to maintain tissue homeostasis under normal conditions. However, how extrinsic signals are transduced into ISCs is poorly understood. Here we reveal that HS is required for Dpp signaling in progenitors to maintain midgut homeostasis under normal conditions.

HSPGs are involved in multiple biological processes, including cell proliferation/differentiation, cell adhesion, extracellular matrix assembly and growth factor diffusion/storage (Esko and Selleck, 2002; Gomes et al., 2013; Iozzo, 1998; Kamimura et al., 2011; Lin, 2004; Lin and Perrimon, 2000; Bernfield et al., 1999; Sarrazin et al., 2011; Yan et al., 2010). The highly diversified functions of HSPGs are mediated by the varied nature of the core proteins and specific HS modifications (Esko and Lindahl, 2001; Esko and Selleck, 2002; Lin, 2004). Although HS plays important roles in the diversified functions of HSPGs, the role of HS in ISC proliferation and differentiation under normal homeostasis has not been systemically explored (Guo et al., 2014; Takemura and Nakato, 2017; You et al., 2014). Our data demonstrate that HS in progenitors negatively regulates ISC proliferation and differentiation to maintain midgut homeostasis under normal conditions (Fig. 1). Consistent with our results, a previous study revealed that heparan sulfate 3-O sulfotransferases (Hs3sts) negatively regulate ISC proliferation (Guo et al., 2014). The extracellular endosulfatases, Sulfs (Sulf1 in *Drosophila*), specifically remove *6-O* sulfate groups (at the *6-O* position of glucosamine residues) from highly sulfated regions of HS. Interestingly, a recent study found that ISC proliferation was increased in the absence of *sulf1* (Takemura and Nakato, 2017). These data indicate that the levels of HS need to be properly controlled for adequate ISC proliferation.

How does HS restrict ISC proliferation? Our data support the notion that under normal conditions, HS is required for Dpp signal activation, which in turn negatively regulates ISC proliferation and differentiation to maintain midgut homeostasis based on the following observations: (1) Dpp signaling was greatly diminished in the absence of HS in ISCs (Figs 1 and 2); (2) Dpp signaling inactivation in progenitors led to increased ISC proliferation and midgut homeostasis loss under normal conditions (Fig. 3); and (3) most importantly, restoring Dpp signaling in the absence of HS in progenitors completely rescued increased ISC proliferation and tissue homeostasis loss (Fig. 5). Although we cannot exclude the possibility that HS may be required for activating other signaling pathways in progenitors, our data favor the notion that HS mainly activates Dpp signaling in progenitors, regardless of the sources of Dpp ligand. Previous studies showed that injury-induced BMP signaling negatively regulates midgut homeostasis; our results indicate that under physiological conditions, Dpp signaling also negatively regulates ISC proliferation and differentiation to maintain tissue homeostasis (Guo et al., 2013; Tian et al., 2017; Zhou et al., 2015). Consistent with previous studies, our results show that Dpp signaling negatively regulates ISC proliferation and differentiation (Guo et al., 2013; Zhou et al., 2015). However, Guo et al.'s, Zhou et al's and our data are contradictory to Tian et al's findings (Tian et al., 2017). We speculate that the paradox may be resulted from the differences in genetic backgrounds, the drivers used and the experimental conditions.

Interestingly, we found that co-expression of *dpp* could completely rescue the defects observed in $esg^{ts}>botv^{RNAi}$ intestines, while co-expression of *gbbGFP* could only partially rescue the defects observed in $esg^{ts}>botv^{RNAi}$ intestines, indicating that Dpp may be more potent than Gbb (Fig. S11). Our finding that HS is required for Dpp signal activation is not unique for ISCs. Previous studies showed that both *sfl* and *dally* are required for Dpp signal activation to control germline stem cell (GSC) maintenance in ovary (Guo and Wang, 2009; Hayashi et al., 2009). Therefore, regardless of the sources of Dpp molecules, we reveal that HS is required for Dpp signal activation to maintain midgut homeostasis under normal conditions.

MATERIALS AND METHODS

Fly lines and cultures

Flies were maintained on standard media at 25°C. Crosses were raised at 18°C in humidity controlled incubators, or as otherwise noted. Flies hatched in 18°C incubators (2–3 days old) were picked and transferred to 29°C incubator, unless otherwise specified. Flies were transferred to new vials with fresh food every day, and dissected at time points specified in the text. In all experiments, only the female posterior midgut was analyzed. Information for alleles and transgenes used in this study can be found either in FlyBase or as noted: *esgGal4, UAS-GFP, tubGal80^{ts}* (esg^{ts}, gift from N. Perrimon, Harvard University), *esgGal4, UAS-RFP, tubGal80^{ts}, sfl^{RNAi}* (BL34601, BL50538), *tubGal80^{ts}, tubGal4* (*tub^{ts}*), *sgl^{RNAi}* (BL65348), *ttv^{RNAi}* (BL51480), *sotv^{RNAi}* (BL52883), *botv^{RNAi}* (GD2083, BL61257), *dally^{RNAi}* (BL33952), *dlp^{RNAi}* (BL34089, BL34091), *Upd1^{RNAi}* (BL33680, BL28722), *Upd2^{RNAi}* (BL33949, BL33988), *Upd3^{RNAi}* (BL32859, BL28575), *GBE+Su(H)-lacZ* (gift from S. Bray, University of Cambridge) (Furriols and Bray, 2001), *10XSTATGFP* (gift from G. Baeg, National University of Singapore) (Bach et al., 2007), *esg-lacZ$^{B7-2-22}$, tubGal4^{ts}*, *Dl^{05151}* (*Dl-lacZ*), *tkv^{RNAi}* (VDRC3059, NIG 14026R-1, and HMS02185), *put^{RNAi}* (GL00069, HMS01944 and NIG 7904R-2), *mad^{RNAi}* (GL01527 and GLV21013), *w(white)^{RNAi}* (BL33623) and/or *Gal4^{RNAi}* (HMS504, from TRiP at Harvard Medical School) were used as control, *FRT40A-tkv^{8}*, *FRT40A-tkv^{a12}*, *UAS-brk, UAS-tkv^{Q253D}* (*tkv^{CA}*), *dally^{P1}* (Nakato et al., 1995), *dally^{06464}* (*dally^{P2}*, BL11685). *hsFlp, ActGal4, UAS-GFP*; *FRT40A-tubGal80* (for MARCM clonal analysis), *UAS-dpp*, *UAS-gbb-GFP* (BL63507 and BL63508).

RNAi knockdown and overexpression experiments

To address gene function in ISCs, *esgGal4, UAS-GFP, tubGal80^{ts}* (esg^{ts}) was used, and crosses (unless stated otherwise) were maintained at 18°C to bypass potential requirements during early developmental stages. 2–3 days old progeny with the desired genotypes were collected after eclosion and maintained at 29°C to inactivate Gal80^{ts} before dissection and immunostaining. The flies were transferred to new vials with fresh food every day. Both *UAS-dsRNA* and *UAS-shRNA* transgene stocks were used in this study. If possible, several dsRNA or shRNA lines were tested for each gene (the lines listed above showed similar phenotypes), and one or two RNAi lines were used for detailed study. To detect JAK/STAT signaling, *esgGal4, UAS-RFP; 10XSTATGFP*, *tubGal80^{ts}* driver was used. The time points that the flies are analyzed/dissected were indicated in the text.

Immunostainings and fluorescence microscopy

For standard immunostaining, intestines were dissected in 1× PBS (10 mM NaH_2PO_4/Na_2HPO_4, 175 mM NaCl, pH 7.4), and fixed in 4% paraformaldehyde for 25 min at room temperature. Samples were rinsed, washed with 1× PBT (0.1% Triton X-100 in 1× PBS) and blocked in 5% horse serum in 1× PBT for 45 min. Embryos were fixed and stained following standard protocol. Primary antibodies were added to the samples and incubated at 4°C overnight. The following primary antibodies were used: mouse mAb anti-Dl [C594.9B, 1:50, developed by S. Artavanis-Tsakonas, Developmental Studies Hybridoma Bank (DSHB)], mouse mAb anti-Prospero (MR1A, 1:100, developed by C.Q. Doe, DSHB), mouse mAb anti-Dlp (13G8, 1:100, developed by P. A. Beachy, DSHB), rabbit mAb anti-pMAD3 (Epitomics, 1:200), rabbit anti-β-glactosidase (Cappel,

1:5000), mouse anti-β-glactosidase (Cell Signaling, 1:1000), rabbit anti-PDM1 (gift from Xaohang Yang, Zhejiang University, 1:1000), rabbit anti-pH3 (pSer10, Millipore, 1:2000, USA) and mouse anti-HS (clone F58-10E4 and F69-3G10, 1:100, Amsbio). For 3G10 staining, fixed intestines were pretreated by heparanase III (2 U/ml, Sigma-Aldrich) at 37°C for 2 h to expose the neo-epitope site. The primary antibodies were detected by fluorescent-conjugated secondary antibodies from Jackson ImmunoResearch Laboratories. Secondary antibodies were incubated for 2 h at room temperature. DAPI (Sigma-Aldrich, 0.1 µg/ml) was added after secondary antibody staining. The samples were mounted in mounting medium (70% glycerol containing 2.5% DABCO). All images were captured by a Zeiss LSM780 inverted confocal microscope, and were processed in Adobe Photoshop and Illustrator.

MARCM ISC clone analysis

The clonal analyses were achieved using the MARCM system. The ISC clones were induced by heat shocking 3–5 day-old adult flies at 37°C for 60 min. The flies were maintained at 25°C incubator and transferred to new vials with fresh food every day. The sizes of the marked clones were assayed at 8 days after clone induction (8D ACI, clones from at least 10 midguts for each genotype were assayed).

Signal quantification

Image-Pro-Plus 6.0 software was used for pMAD signal quantification. Two parameters, integrated optical density (IOD) and area, were used in the analysis. For pMAD signal quantification in ISCs, a pixel filter was set to ensure that the area of interest did not include objects larger than 20 pixels, excluding esg^- cells (which are ECs and ee cells). IOD value per ISC was used. At least four different images were analyzed for each sample.

qRT-PCR

RNA was extracted from 30 flies or guts using TRIzol (Invitrogen). RNA was cleaned using RNAeasy (QIAGEN), and complementary DNA (cDNA) was synthesized using the iScript cDNA synthesis kit (Bio-Rad). Quantitative PCR was performed using the iScript one-step RT-PCR SYBR green kit (Bio-Rad). Data were acquired using an iQ5 System (Bio-Rad). qRT-PCR was performed in duplicate on each of three independent biological replicates. All results are presented as mean±s.d. of the biological replicates. The ribosomal gene *RpL11* was used as the normalization control. Primers used for qRT-PCR can be found in Table S1.

Data analysis

pH3 numbers were scored manually under Zeiss Imager Z2/LSM780 microscope for indicated genotypes. To determine the relative number of esg^+ cells per confocal image (including *esg>GFP*$^+$, *esg-lacZ*$^+$ and *10xSTATGFP*$^+$), confocal images of 40× lens/1.0 zoom from a defined posterior midgut region (R4-R5 regions) of different genotypes indicated were acquired. The relative number of esg^+ and *GBE+Su(H)-lacZ*$^+$ cells was determined using Image-Pro Plus software from each confocal image. The number of intestines scored is indicated in the text. Fluorescence intensity of *10xSTATGFP* and HS was measured using Image Pro Plus 6.0 (measure/count function). The data are presented as the means±standard deviation and two-tailed Student's *t*-tests were performed for statistical comparisons. PEMS 3.1 software was used for s.d. analyses and Sigma Plot software for graph generation. *P<0.05; **P<0.01. The graphs were further modified using Adobe Photoshop and Illustrator.

Acknowledgements

We are grateful to Norbert Perrimon, Sarah Bray, Xinhua Lin, Steven Hou, Gyeong-Hun Baeg, Rongwen Xi, Xiaohang Yang and Yu Cai for generous gifts of reagents; the Bloomington Stock Center, VDRC, NIG-FLY Center, TRiP at Harvard Medical School (NIH/NIGMS R01-GM084947) and Tsinghua Fly Center (THFC) for fly stocks; and DSHB for antibodies. We apologize to the colleagues whose work could not be cited because of space restrictions.

Competing interests

The authors declare no competing or financial interests.

Author contributions

Conceptualization: Z.L.; Methodology: R.K., L.S.; Formal analysis: H.M., Huiqing Zhao, F.L., R.K., Z.L.; Investigation: H.M., Huiqing Zhao, F.L., Hang Zhao, R.K., L.S., M.W.; Data curation: Z.L.; Writing - original draft: Z.L.; Writing - review & editing: Z.L.; Supervision: Z.L.; Project administration: Z.L.; Funding acquisition: Z.L.

Funding

This work is supported by grants from the National Natural Science Foundation of China (nos. 31471384, 31972893 and 31271582), and the Beijing Natural Science Foundation (nos. KZ201910028040 and 5162004).

Data availability

The datasets generated and/or analyzed during the current study are available from the corresponding author on reasonable request.

Supplementary information

Supplementary information available online at
http://bio.biologists.org/lookup/doi/10.1242/bio.047126.supplemental

References

Amcheslavsky, A., Jiang, J. and Ip, Y. T. (2009). Tissue damage-induced intestinal stem cell division in *Drosophila*. *Cell Stem Cell* **4**, 49-61. doi:10.1016/j.stem.2008.10.016

Bach, E. A., Ekas, L. A., Ayala-Camargo, A., Flaherty, M. S., Lee, H., Perrimon, N. and Baeg, G.-H. (2007). GFP reporters detect the activation of the *Drosophila* JAK/STAT pathway *in vivo*. *Gene Expr. Patterns* **7**, 323-331. doi:10.1016/j.modgep.2006.08.003

Beebe, K., Lee, W.-C. and Micchelli, C. A. (2010). JAK/STAT signaling coordinates stem cell proliferation and multilineage differentiation in the *Drosophila* intestinal stem cell lineage. *Dev. Biol.* **338**, 28-37. doi:10.1016/j.ydbio.2009.10.045

Belenkaya, T. Y., Han, C., Yan, D., Opoka, R. J., Khodoun, M., Liu, H. and Lin, X. (2004). *Drosophila* Dpp morphogen movement is independent of dynamin-mediated endocytosis but regulated by the glypican members of heparan sulfate proteoglycans. *Cell* **119**, 231-244. doi:10.1016/j.cell.2004.09.031

Bellaiche, Y., The, I. and Perrimon, N. (1998). Tout-velu is a Drosophila homologue of the putative tumour suppressor EXT-1 and is needed for Hh diffusion. *Nature* **394**, 85. doi:10.1038/27932

Bernfield, M., Götte, M., Park, P. W., Reizes, O., Fitzgerald, M. L., Lincecum, J. and Zako, M. (1999). Functions of cell surface Heparan sulfate proteoglycans. *Annu. Rev. Biochem.* **68**, 729-777. doi:10.1146/annurev.biochem.68.1.729

Binari, R. C., Staveley, B. E., Johnson, W. A., Godavarti, R., Sasisekharan, R. and Manoukian, A. S. (1997). Genetic evidence that heparin-like glycosaminoglycans are involved in wingless signaling. *Development* **124**, 2623-2632.

Biteau, B. and Jasper, H. (2011). EGF signaling regulates the proliferation of intestinal stem cells in *Drosophila*. *Development* **138**, 1045-1055. doi:10.1242/dev.056671

Biteau, B. and Jasper, H. (2014). Slit/Robo signaling regulates cell fate decisions in the intestinal stem cell lineage of *Drosophila*. *Cell Rep.* **7**, 1867-1875. doi:10.1016/j.celrep.2014.05.024

Bornemann, D. J., Duncan, J. E., Staatz, W., Selleck, S. and Warrior, R. (2004). Abrogation of heparan sulfate synthesis in *Drosophila* disrupts the Wingless, Hedgehog and Decapentaplegic signaling pathways. *Development* **131**, 1927-1938. doi:10.1242/dev.01061

Brawley, C. and Matunis, E. (2004). Regeneration of male germline stem cells by spermatogonial dedifferentiation *in vivo*. *Science* **304**, 1331-1334. doi:10.1126/science.1097676

Buchon, N., Broderick, N. A., Chakrabarti, S. and Lemaitre, B. (2009). Invasive and indigenous microbiota impact intestinal stem cell activity through multiple pathways in *Drosophila*. *Genes Dev.* **23**, 2333-2344. doi:10.1101/gad.1827009

Casali, A. and Batlle, E. (2009). Intestinal stem cells in mammals and *Drosophila*. *Cell Stem Cell* **4**, 124-127. doi:10.1016/j.stem.2009.01.009

Chakrabarti, S., Dudzic, J. P., Li, X., Collas, E. J., Boquete, J.-P. and Lemaitre, B. (2016). Remote control of intestinal stem cell activity by haemocytes in *Drosophila*. *PLoS Genet.* **12**, e1006089. doi:10.1371/journal.pgen.1006089

Chen, J., Xu, N., Huang, H., Cai, T. and Xi, R. (2016). A feedback amplification loop between stem cells and their progeny promotes tissue regeneration and tumorigenesis. *eLife* **5**, e14330. doi:10.7554/eLife.14330

Chen, J., Xu, N., Wang, C., Huang, P., Huang, H., Jin, Z., Yu, Z., Cai, T., Jiao, R. and Xi, R. (2018). Transient Scute activation via a self-stimulatory loop directs enteroendocrine cell pair specification from self-renewing intestinal stem cells. *Nat. Cell Biol.* **20**, 152-161. doi:10.1038/s41556-017-0020-0

Choi, N. H., Lucchetta, E. and Ohlstein, B. (2011). Nonautonomous regulation of *Drosophila* midgut stem cell proliferation by the insulin-signaling pathway. *Proc. Natl. Acad. Sci. USA* **108**, 18702-18707. doi:10.1073/pnas.1109348108

Cordero, J. B., Stefanatos, R. K., Scopelliti, A., Vidal, M. and Sansom, O. J. (2012). Inducible progenitor-derived Wingless regulates adult midgut

regeneration in *Drosophila*. *EMBO J.* **31**, 3901-3917. doi:10.1038/emboj.2012.248

Dani, N., Nahm, M., Lee, S. and Broadie, K. (2012). A targeted glycan-related gene screen reveals heparan sulfate proteoglycan sulfation regulates WNT and BMP trans-synaptic signaling. *PLoS Genet.* **8**, e1003031. doi:10.1371/journal.pgen.1003031

de Navascués, J., Perdigoto, C. N., Bian, Y., Schneider, M. H., Bardin, A. J., Martínez-Arias, A. and Simons, B. D. (2012). *Drosophila* midgut homeostasis involves neutral competition between symmetrically dividing intestinal stem cells. *EMBO J.* **31**, 2473-2485. doi:10.1038/emboj.2012.106

Edgar, B. A. (2012). Intestinal stem cells: no longer immortal but ever so clever. *EMBO J.* **31**, 2441-2443. doi:10.1038/emboj.2012.133

Esko, J. D. and Lindahl, U. (2001). Molecular diversity of heparan sulfate. *J. Clin. Invest.* **108**, 169-173. doi:10.1172/JCI200113530

Esko, J. D. and Selleck, S. B. (2002). Order out of chaos: assembly of ligand binding sites in Heparan sulfate. *Annu. Rev. Biochem.* **71**, 435-471. doi:10.1146/annurev.biochem.71.110601.135458

Filmus, J., Capurro, M. and Rast, J. (2008). Glypicans. *Genome Biol.* **9**, 224. doi:10.1186/gb-2008-9-5-224

Fujise, M., Takeo, S., Kamimura, K., Matsuo, T., Aigaki, T., Izumi, S. and Nakato, H. (2003). Dally regulates Dpp morphogen gradient formation in the *Drosophila* wing. *Development* **130**, 1515-1522. doi:10.1242/dev.00379

Furriols, M. and Bray, S. (2001). A model Notch response element detects Suppressor of Hairless-dependent molecular switch. *Curr. Biol.* **11**, 60-64. doi:10.1016/S0960-9822(00)00044-0

Gomes, A. M., Stelling, M. P. and Pavão, M. S. G. (2013). Heparan sulfate and heparanase as modulators of breast cancer progression. *BioMed Res. Int.* **2013**, 11. doi:10.1155/2013/852093

Goulas, S., Conder, R. and Knoblich, J. A. (2012). The Par complex and integrins direct asymmetric cell division in adult intestinal stem cells. *Cell Stem Cell* **11**, 529-540. doi:10.1016/j.stem.2012.06.017

Guo, Z. and Ohlstein, B. (2015). Bidirectional Notch signaling regulates *Drosophila* intestinal stem cell multipotency. *Science* **350**. doi:10.1126/science.aab0988

Guo, Z. and Wang, Z. (2009). The glypican Dally is required in the niche for the maintenance of germline stem cells and short-range BMP signaling in the *Drosophila* ovary. *Development* **136**, 3627-3635. doi:10.1242/dev.036939

Guo, Z., Driver, I. and Ohlstein, B. (2013). Injury-induced BMP signaling negatively regulates *Drosophila* midgut homeostasis. *J. Cell Biol.* **201**, 945-961. doi:10.1083/jcb.201302049

Guo, Y., Li, Z. and Lin, X. (2014). Hs3st-A and Hs3st-B regulate intestinal homeostasis in *Drosophila* adult midgut. *Cell. Signal.* **26**, 2317-2325. doi:10.1016/j.cellsig.2014.07.015

Han, C., Belenkaya, T. Y., Khodoun, M., Tauchi, M., Lin, X. and Lin, X. (2004). Distinct and collaborative roles of *Drosophila* EXT family proteins in morphogen signalling and gradient formation. *Development* **131**, 1563-1575. doi:10.1242/dev.01051

Han, H., Pan, C., Liu, C., Lv, X., Yang, X., Xiong, Y., Lu, Y., Wu, W., Han, J., Zhou, Z. et al. (2015). Gut–neuron interaction via Hh signaling regulates intestinal progenitor cell differentiation in *Drosophila*. *Cell Discov.* **1**, 15006. doi:10.1038/celldisc.2015.6

Hayashi, Y., Kobayashi, S. and Nakato, H. (2009). *Drosophila* glypicans regulate the germline stem cell niche. *J. Cell Biol.* **187**, 473-480. doi:10.1083/jcb.200904118

Iozzo, R. V. (1998). Matrix proteoglycans: from molecular design to cellular function. *Annu. Rev. Biochem.* **67**, 609-652. doi:10.1146/annurev.biochem.67.1.609

Jackson, S. M., Nakato, H., Sugiura, M., Jannuzi, A., Oakes, R., Kaluza, V., Golden, C. and Selleck, S. B. (1997). dally, a Drosophila glypican, controls cellular responses to the TGF-beta-related morphogen, Dpp. *Development* **124**, 4113-4120.

Jaźwińska, A., Kirov, N., Wieschaus, E., Roth, S. and Rushlow, C. (1999). The *Drosophila* gene brinker reveals a novel mechanism of Dpp target gene regulation. *Cell* **96**, 563-573. doi:10.1016/S0092-8674(00)80660-1

Jiang, H. and Edgar, B. A. (2009). EGFR signaling regulates the proliferation of *Drosophila* adult midgut progenitors. *Development* **136**, 483-493. doi:10.1242/dev.026955

Jiang, H., Patel, P. H., Kohlmaier, A., Grenley, M. O., McEwen, D. G. and Edgar, B. A. (2009). Cytokine/Jak/Stat signaling mediates regeneration and homeostasis in the *Drosophila* midgut. *Cell* **137**, 1343-1355. doi:10.1016/j.cell.2009.05.014

Jiang, H., Grenley, M. O., Bravo, M.-J., Blumhagen, R. Z. and Edgar, B. A. (2011). EGFR/Ras/MAPK signaling mediates adult midgut epithelial homeostasis and regeneration in *Drosophila*. *Cell Stem Cell* **8**, 84-95. doi:10.1016/j.stem.2010.11.026

Jin, Y., Patel, P. H., Kohlmaier, A., Pavlovic, B., Zhang, C. and Edgar, B. A. (2017). Intestinal stem cell pool regulation in *Drosophila*. *Stem Cell Rep.* **8**, 1479-1487. doi:10.1016/j.stemcr.2017.04.002

Kamimura, K., Koyama, T., Habuchi, H., Ueda, R., Masu, M., Kimata, K. and Nakato, H. (2006). Specific and flexible roles of heparan sulfate modifications in *Drosophila* FGF signaling. *J. Cell Biol.* **174**, 773-778. doi:10.1083/jcb.200603129

Kamimura, K., Maeda, N. and Nakato, H. (2011). In vivo manipulation of heparan sulfate structure and its effect on *Drosophila* development. *Glycobiology* **21**, 607-618. doi:10.1093/glycob/cwq202

Karpowicz, P., Perez, J. and Perrimon, N. (2010). The Hippo tumor suppressor pathway regulates intestinal stem cell regeneration. *Development* **137**, 4135-4145. doi:10.1242/dev.060483

Lee, T. and Luo, L. (2001). Mosaic analysis with a repressible cell marker (MARCM) for *Drosophila* neural development. *Trends Neurosci.* **24**, 251-254. doi:10.1016/S0166-2236(00)01791-4

Lee, W.-C., Beebe, K., Sudmeier, L. and Micchelli, C. A. (2009). Adenomatous polyposis coli regulates *Drosophila* intestinal stem cell proliferation. *Development* **136**, 2255-2264. doi:10.1242/dev.035196

Levings, D. C. and Nakato, H. (2017). Loss of heparan sulfate in the niche leads to tumor-like germ cell growth in the *Drosophila* testis. *Glycobiology* **28**, 32-41. doi:10.1093/glycob/cwx090

Li, H., Qi, Y. and Jasper, H. (2013a). Dpp signaling determines regional stem cell identity in the regenerating adult *Drosophila* gastrointestinal tract. *Cell Rep.* **4**, 10-18. doi:10.1016/j.celrep.2013.05.040

Li, Z., Zhang, Y., Han, L., Shi, L. and Lin, X. (2013b). Trachea-derived Dpp controls adult midgut homeostasis in *Drosophila*. *Dev. Cell* **24**, 133-143. doi:10.1016/j.devcel.2012.12.010

Li, Z., Guo, Y., Han, L., Zhang, Y., Shi, L., Huang, X. and Lin, X. (2014). Debra-mediated Ci degradation controls tissue homeostasis in *Drosophila* adult midgut. *Stem Cell Rep.* **2**, 135-144. doi:10.1016/j.stemcr.2013.12.011

Lin, X. (2004). Functions of heparan sulfate proteoglycans in cell signaling during development. *Development* **131**, 6009-6021. doi:10.1242/dev.01522

Lin, H. (2008). Cell biology of stem cells: an enigma of asymmetry and self-renewal. *J. Cell Biol.* **180**, 257-260. doi:10.1083/jcb.200712159

Lin, X. and Perrimon, N. (1999). Dally cooperates with *Drosophila* Frizzled 2 to transduce Wingless signalling. *Nature* **400**, 281. doi:10.1038/22343

Lin, X. and Perrimon, N. (2000). Role of heparan sulfate proteoglycans in cell-cell signaling in *Drosophila*. *Matrix Biol.* **19**, 303-307. doi:10.1016/S0945-053X(00)00073-1

Lin, X. and Perrimon, N. (2002). Developmental roles of heparan sulfate proteoglycans in *Drosophila*. *Glycoconj. J.* **19**, 363-368. doi:10.1023/A:1025329323438

Lin, G. and Xi, R. (2008). Intestinal stem cell, muscular niche and Wingless signaling. *Fly (Austin)* **2**, 310-312. doi:10.4161/fly.7428

Lin, G., Xu, N. and Xi, R. (2008). Paracrine Wingless signalling controls self-renewal of *Drosophila* intestinal stem cells. *Nature* **455**, 1119-1123. doi:10.1038/nature07329

Liu, M., Lim, T. M. and Cai, Y. (2010). The *Drosophila* female germline stem cell lineage acts to spatially restrict DPP function within the Niche. *Sci. Signal.* **3**, ra57. doi:10.1126/scisignal.2000740

Lu, Y. and Li, Z. (2015). No intestinal stem cell regeneration after complete progenitor ablation in Drosophila adult midgut. *J. Genet. Genomics* **42**, 83-86. doi:10.1016/j.jgg.2014.10.002

Martorell, Ò., Barriga, F. M., Merlos-Suárez, A., Stephan-Otto Attolini, C., Casanova, J., Batlle, E., Sancho, E. and Casali, A. (2014). Iro/IRX transcription factors negatively regulate Dpp/TGF-β pathway activity during intestinal tumorigenesis. *EMBO Rep.* **15**, 1210-1218. doi:10.15252/embr.201438622

Micchelli, C. A. and Perrimon, N. (2006). Evidence that stem cells reside in the adult *Drosophila* midgut epithelium. *Nature* **439**, 475-479. doi:10.1038/nature04371

Mii, Y., Yamamoto, T., Takada, R., Mizumoto, S., Matsuyama, M., Yamada, S., Takada, S. and Taira, M. (2017). Roles of two types of heparan sulfate clusters in Wnt distribution and signaling in *Xenopus*. *Nat. Commun.* **8**, 1973. doi:10.1038/s41467-017-02076-0

Morrison, S. J. and Spradling, A. C. (2008). Stem cells and niches: mechanisms that promote stem cell maintenance throughout life. *Cell* **132**, 598-611. doi:10.1016/j.cell.2008.01.038

Nakato, H., Futch, T. A. and Selleck, S. B. (1995). The division abnormally delayed, dally, gene: a putative integral membrane proteoglycan required for cell division patterning during postembryonic development of the nervous system in *Drosophila*. *Development* **121**, 3687-3702.

O'Brien, Lucy, E., Soliman, S. S., Li, X. and Bilder, D. (2011). Altered modes of stem cell division drive adaptive intestinal growth. *Cell* **147**, 603-614. doi:10.1016/j.cell.2011.08.048

Ohlstein, B. and Spradling, A. (2006). The adult *Drosophila* posterior midgut is maintained by pluripotent stem cells. *Nature* **439**, 470-474. doi:10.1038/nature04333

Ohlstein, B. and Spradling, A. (2007). Multipotent *Drosophila* intestinal stem cells specify daughter cell fates by differential Notch signaling. *Science* **315**, 988-992. doi:10.1126/science.1136606

Perdigoto, C. N., Schweisguth, F. and Bardin, A. J. (2011). Distinct levels of Notch activity for commitment and terminal differentiation of stem cells in the adult fly intestine. *Development* **138**, 4585-4595. doi:10.1242/dev.065292

Radtke, F. and Clevers, H. (2005). Self-renewal and cancer of the gut: two sides of a coin. *Science* **307**, 1904-1909. doi:10.1126/science.1104815

Raff, M. (2003). Adult stem cell plasticity: fact or artifact? *Annu. Rev. Cell Dev. Biol.* **19**, 1-22. doi:10.1146/annurev.cellbio.19.111301.143037

Rahman, M. M., Franch-Marro, X., Maestro, J. L., Martin, D. and Casali, A. (2017). Local Juvenile Hormone activity regulates gut homeostasis and tumor growth in adult *Drosophila*. *Sci. Rep.* **7**, 11677. doi:10.1038/s41598-017-11199-9

Ren, F., Wang, B., Yue, T., Yun, E.-Y., Ip, Y. T. and Jiang, J. (2010). Hippo signaling regulates *Drosophila* intestine stem cell proliferation through multiple pathways. *Proc. Natl. Acad. Sci. USA* **107**, 21064-21069. doi:10.1073/pnas.1012759107

Ren, W., Zhang, Y., Li, M., Wu, L., Wang, G., Baeg, G.-H., You, J., Li, Z. and Lin, X. (2015). Windpipe controls *Drosophila* intestinal homeostasis by regulating JAK/STAT pathway via promoting receptor endocytosis and lysosomal degradation. *PLoS Genet.* **11**, e1005180. doi:10.1371/journal.pgen.1005180

Sarrazin, S., Lamanna, W. C. and Esko, J. D. (2011). Heparan sulfate proteoglycans. *Cold Spring Harb. Perspect. Biol.* **3**, a004952. doi:10.1101/cshperspect.a004952

Schell, J. C., Wisidagama, D. R., Bensard, C., Zhao, H., Wei, P., Tanner, J., Flores, A., Mohlman, J., Sorensen, L. K., Earl, C. S. et al. (2017). Control of intestinal stem cell function and proliferation by mitochondrial pyruvate metabolism. *Nat. Cell Biol.* **19**, 1027. doi:10.1038/ncb3593

Shaw, R. L., Kohlmaier, A., Polesello, C., Veelken, C., Edgar, B. A. and Tapon, N. (2010). The Hippo pathway regulates intestinal stem cell proliferation during *Drosophila* adult midgut regeneration. *Development* **137**, 4147-4158. doi:10.1242/dev.052506

Singh, S. R., Zeng, X., Zhao, J., Liu, Y., Hou, G., Liu, H. and Hou, S. X. (2016). The lipolysis pathway sustains normal and transformed stem cells in adult Drosophila. *Nature* **538**, 109. doi:10.1038/nature19788

Stainier, D. Y. R. (2005). No organ left behind: tales of gut development and evolution. *Science* **307**, 1902-1904. doi:10.1126/science.1108709

Staley, B. K. and Irvine, K. D. (2010). Warts and Yorkie mediate intestinal regeneration by influencing stem cell proliferation. *Curr. Biol.* **20**, 1580-1587. doi:10.1016/j.cub.2010.07.041

Takei, Y., Ozawa, Y., Sato, M., Watanabe, A. and Tabata, T. (2004). Three *Drosophila* EXT genes shape morphogen gradients through synthesis of heparan sulfate proteoglycans. *Development* **131**, 73-82. doi:10.1242/dev.00913

Takemura, M. and Nakato, H. (2017). *Drosophila* Sulf1 is required for the termination of intestinal stem cell division during regeneration. *J. Cell Sci.* **130**, 332-343. doi:10.1242/jcs.195305

Tian, A. and Jiang, J. (2014). Intestinal epithelium-derived BMP controls stem cell self-renewal in *Drosophila* adult midgut. *eLife* **3**, e01857. doi:10.7554/eLife.01857

Tian, A., Shi, Q., Jiang, A., Li, S., Wang, B. and Jiang, J. (2015). Injury-stimulated Hedgehog signaling promotes regenerative proliferation of *Drosophila* intestinal stem cells. *J. Cell Biol.* **208**, 807-819. doi:10.1083/jcb.201409025

Tian, A., Wang, B. and Jiang, J. (2017). Injury-stimulated and self-restrained BMP signaling dynamically regulates stem cell pool size during *Drosophila* midgut regeneration. *Proc. Natl. Acad. Sci. USA* **114**, E2699-E2708. doi:10.1073/pnas.1617790114

Toyoda, H., Kinoshita-Toyoda, A., Fox, B. and Selleck, S. B. (2000a). Structural analysis of Glycosaminoglycans in animals bearing mutations in sugarless, sulfateless, and tout-velu: *Drosophila* homologues of vertebrate genes encoding glycosaminoglycan biosynthetic enzymes. *J. Biol. Chem.* **275**, 21856-21861. doi:10.1074/jbc.M003540200

Toyoda, H., Kinoshita-Toyoda, A. and Selleck, S. B. (2000b). Structural analysis of glycosaminoglycans in *Drosophila* and *Caenorhabditis elegans* and demonstration that tout-velu, a *Drosophila* gene related to EXT tumor suppressors, affects Heparan sulfate *in vivo*. *J. Biol. Chem.* **275**, 2269-2275. doi:10.1074/jbc.275.4.2269

Wang, P. and Hou, S. X. (2010). Regulation of intestinal stem cells in mammals and *Drosophila*. *J. Cell. Physiol.* **222**, 33-37. doi:10.1002/jcp.21928

Xie, T. and Spradling, A. C. (1998). Decapentaplegic is essential for the maintenance and division of germline stem cells in the *Drosophila* ovary. *Cell* **94**, 251-260. doi:10.1016/S0092-8674(00)81424-5

Xu, N., Wang, S. Q., Tan, D., Gao, Y., Lin, G. and Xi, R. (2011). EGFR, Wingless and JAK/STAT signaling cooperatively maintain *Drosophila* intestinal stem cells. *Dev. Biol.* **354**, 31-43. doi:10.1016/j.ydbio.2011.03.018

Xu, R., Li, J., Zhao, H., Kong, R., Wei, M., Shi, L., Bai, G. and Li, Z. (2018). Self-restrained regulation of stem cell niche activity by niche components in the *Drosophila* testis. *Dev. Biol.* **439**, 42-51. doi:10.1016/j.ydbio.2018.04.011

Yan, D. and Lin, X. (2009). Shaping morphogen gradients by proteoglycans. *Cold Spring Harb. Perspect. Biol.* **1**, a002493. doi:10.1101/cshperspect.a002493

Yan, D., Wu, Y., Yang, Y., Belenkaya, T. Y., Tang, X. and Lin, X. (2010). The cell-surface proteins Dally-like and Ihog differentially regulate Hedgehog signaling strength and range during development. *Development* **137**, 2033-2044. doi:10.1242/dev.045740

Yeung, T. M., Chia, L. A., Kosinski, C. M. and Kuo, C. J. (2011). Regulation of self-renewal and differentiation by the intestinal stem cell niche. *Cell. Mol. Life Sci.* **68**, 2513-2523. doi:10.1007/s00018-011-0687-5

You, J., Zhang, Y., Li, Z., Lou, Z., Jin, L. and Lin, X. (2014). *Drosophila* perlecan regulates intestinal stem cell activity via cell-matrix attachment. *Stem Cell Rep.* **2**, 761-769. doi:10.1016/j.stemcr.2014.04.007

Yu, C., Griffiths, L. R. and Haupt, L. M. (2017). Exploiting Heparan sulfate proteoglycans in human neurogenesis—controlling lineage specification and fate. *Front. Integr. Neurosci.* **11**. doi:10.3389/fnint.2017.00028

Zeng, X., Han, L., Singh, S. R., Liu, H., Neumüller, R. A., Yan, D., Hu, Y., Liu, Y., Liu, W., Lin, X. et al. (2015). Genome-wide RNAi screen identifies networks involved in intestinal stem cell regulation in *Drosophila*. *Cell Rep.* **10**, 1226-1238. doi:10.1016/j.celrep.2015.01.051

Zhai, Z., Boquete, J.-P. and Lemaitre, B. (2017). A genetic framework controlling the differentiation of intestinal stem cells during regeneration in *Drosophila*. *PLoS Genet.* **13**, e1006854. doi:10.1371/journal.pgen.1006854

Zhang, Y., You, J., Ren, W. and Lin, X. (2013). *Drosophila* glypicans Dally and Dally-like are essential regulators for JAK/STAT signaling and Unpaired distribution in eye development. *Dev. Biol.* **375**, 23-32. doi:10.1016/j.ydbio.2012.12.019

Zhou, J., Florescu, S., Boettcher, A.-L., Luo, L., Dutta, D., Kerr, G., Cai, Y., Edgar, B. A. and Boutros, M. (2015). Dpp/Gbb signaling is required for normal intestinal regeneration during infection. *Dev. Biol.* **399**, 189-203. doi:10.1016/j.ydbio.2014.12.017

Supplementary material

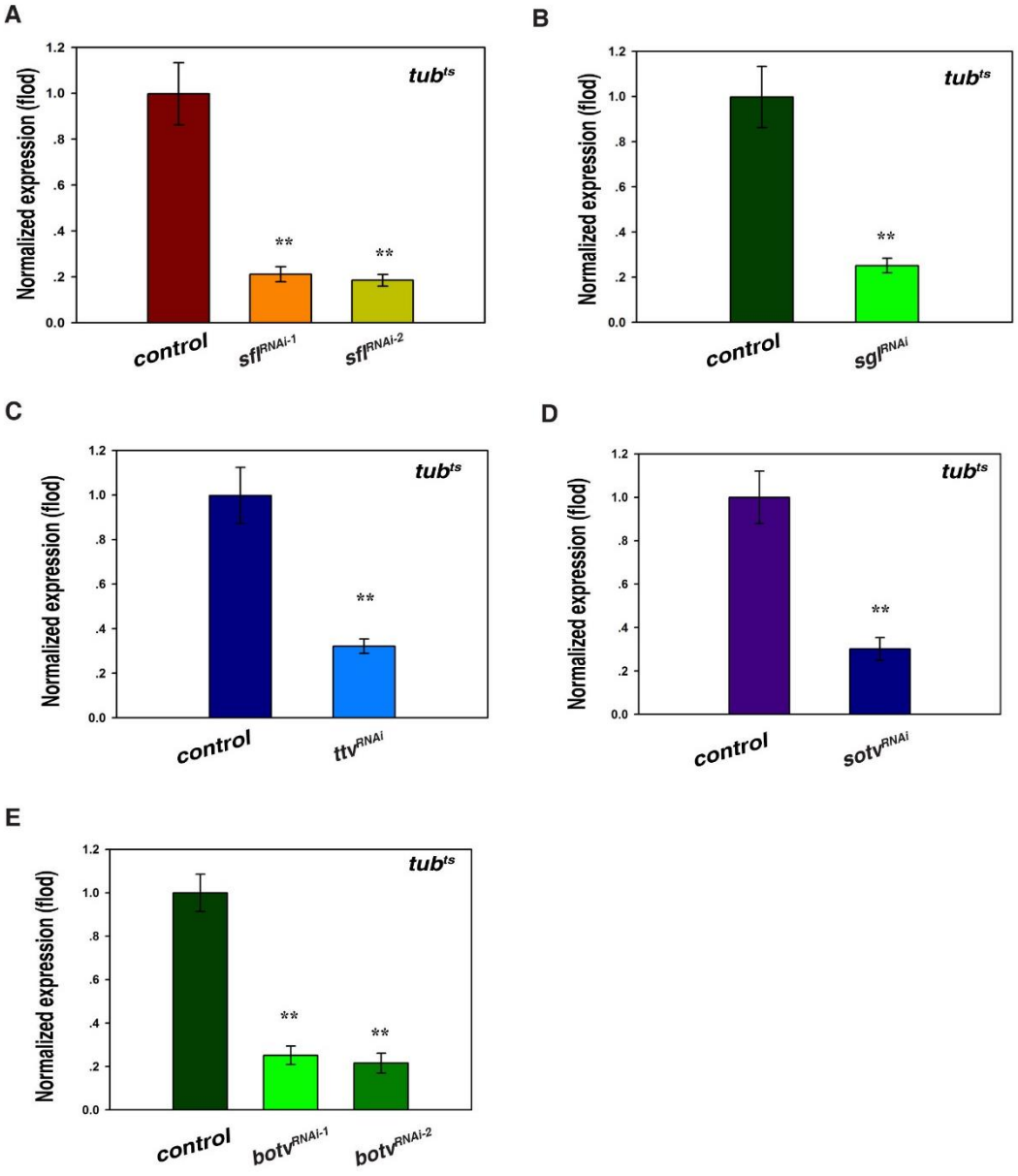

Fig.S1. Knockdown efficacy of RNAi lines against genes encoding enzymes in HS chain biogenesis. (A) Knockdown efficacy of two different *sfl* RNAi lines used in this study was determined by qRT-PCR quantification from $tub^{ts}>sfl^{RNAi}$ flies (ovaries were not included). Ribosomal gene *RpL11* was used as normalization control. means ± SD are shown. $^{**}p < 0.01$. (B) Knockdown efficacy of *sgl* RNAi line used in this study was determined by qRT-PCR quantification from $tub^{ts}>sgl^{RNAi}$ flies (ovaries were not included). Ribosomal gene *RpL11* was used as normalization control. means ± SD are shown. $^{**}p < 0.01$. (C) Knockdown efficacy of *ttv* RNAi line used in this study was determined by qRT-PCR quantification from $tub^{ts}>ttv^{RNAi}$ flies (ovaries were not included). Ribosomal gene *RpL11* was used as normalization control. means ± SD are shown. $^{**}p < 0.01$. (D) Knockdown efficacy of *sotv* RNAi line used in this study was determined by qRT-PCR quantification from $tub^{ts}>sotv^{RNAi}$ flies (ovaries were not included). Ribosomal gene *RpL11* was used as normalization control. means ± SD are shown. $^{**}p < 0.01$. (E) Knockdown efficacy of two different *botv* RNAi lines used in this study was determined by qRT-PCR quantification from $tub^{ts}>botv^{RNAi}$ flies (ovaries were not included). Ribosomal gene *RpL11* was used as normalization control. means ± SD are shown. $^{**}p < 0.01$.

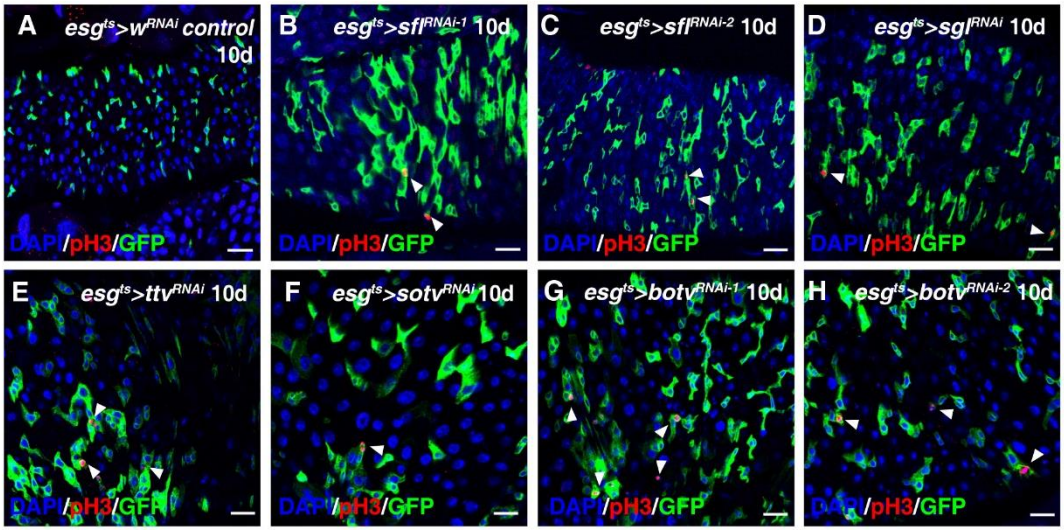

Fig. S2. ISC proliferation is increased upon loss of HS in progenitors. (A) pH3 (red) in control intestines. (B) pH3 (red) in *esg*^{ts}>*sfl*$^{RNAi\text{-}1}$ intestines (white arrowheads). (**C)** pH3 (red) in *esg*^{ts}>*sfl*$^{RNAi\text{-}2}$ intestines (white arrowheads). (D) pH3 (red) in *esg*^{ts}>*sgl*^{RNAi} intestines (white arrowheads). (E) pH3 (red) in *esg*^{ts}>*ttv*^{RNAi} intestines (white arrowheads). (F) pH3 (red) in *esg*^{ts}>*sotv*^{RNAi} intestines (white arrowhead). (G) pH3 (red) in *esg*^{ts}>*botv*$^{RNAi\text{-}1}$ intestines (white arrowheads). (H) pH3 (red) in *esg*^{ts}>*botv*$^{RNAi\text{-}2}$ intestines (white arrowheads). GFP in green, blue indicates DAPI staining for DNA. Scale bars: 20 μm. Please refer to Fig. 1J for quantification data.

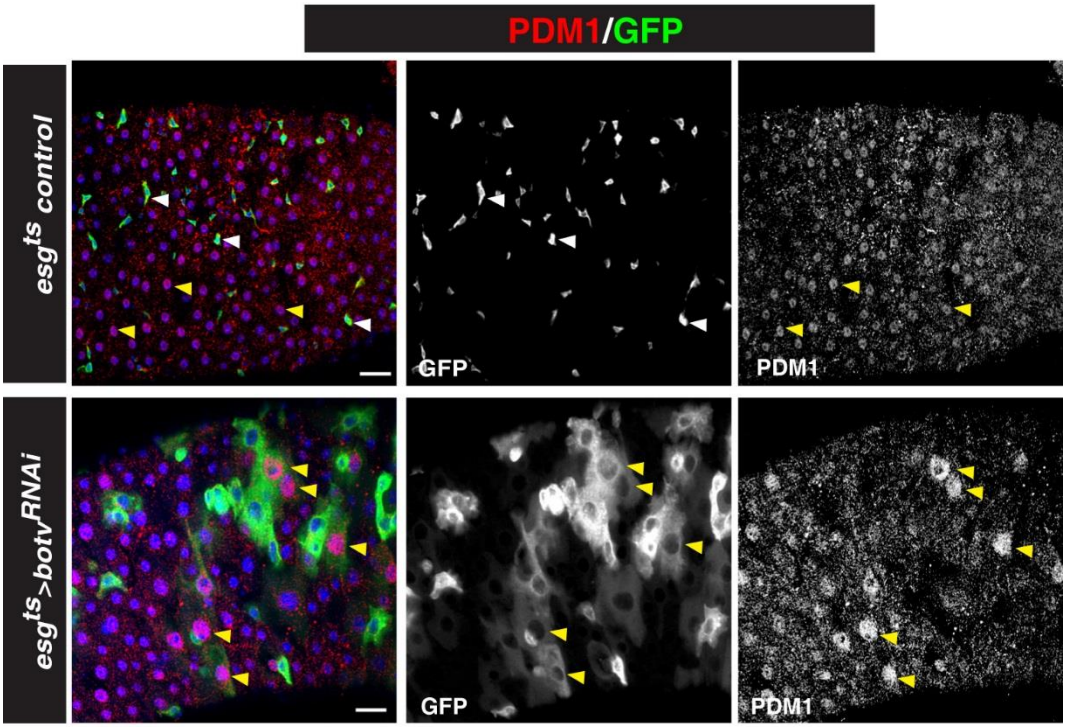

Fig. S3. Depletion of HS in progenitors results in intestinal homeostasis loss. (Upper panel) progenitors (green) and mature ECs (by PDM1, red) in control intestines (white and yellow arrowheads). (Lower panel) Many large *esg*$^{+}$ cells express mature EC-marker PDM1 (red) in *esg*^{ts}>*botv*^{RNAi} intestines (yellow arrowheads). Split channel for GFP and PDM1 was shown. GFP in green, blue indicates DAPI staining for DNA. Scale bars: 20 μm.

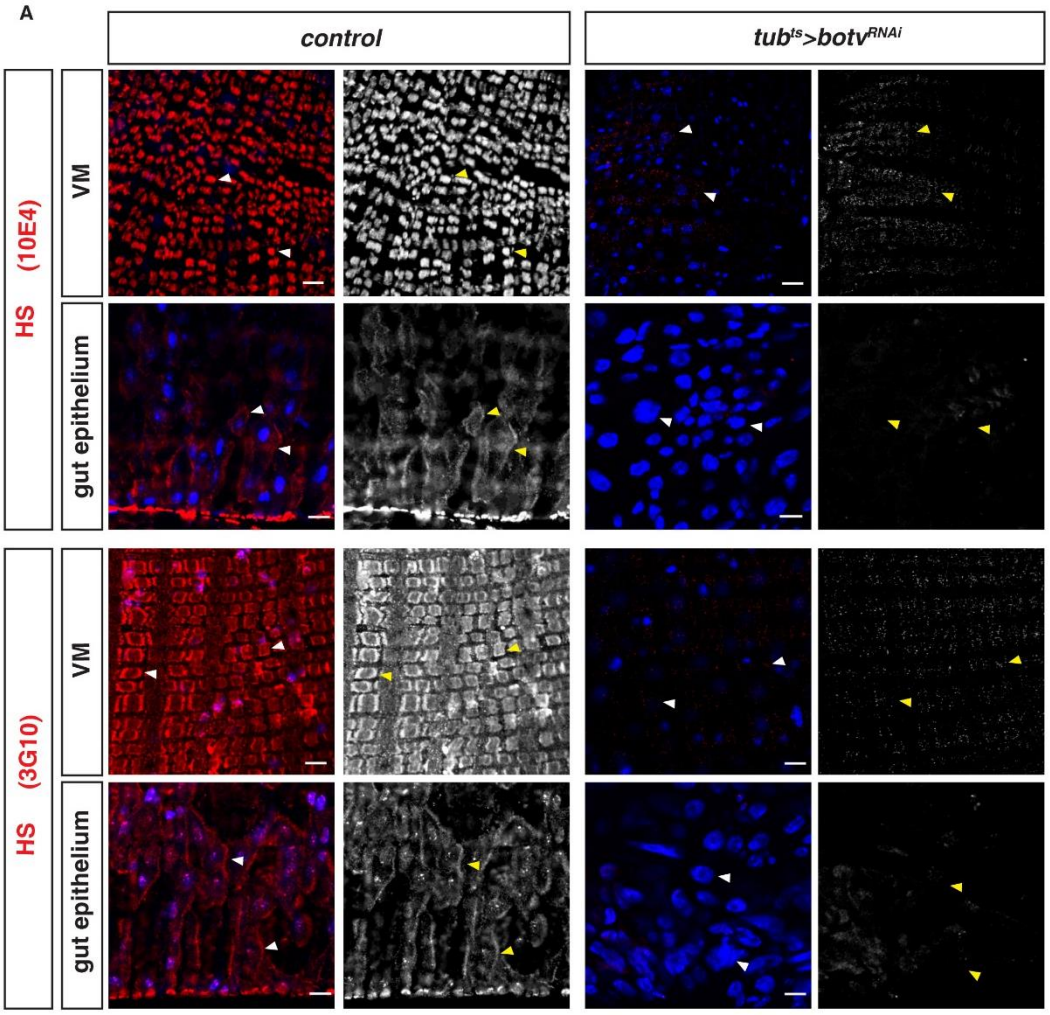

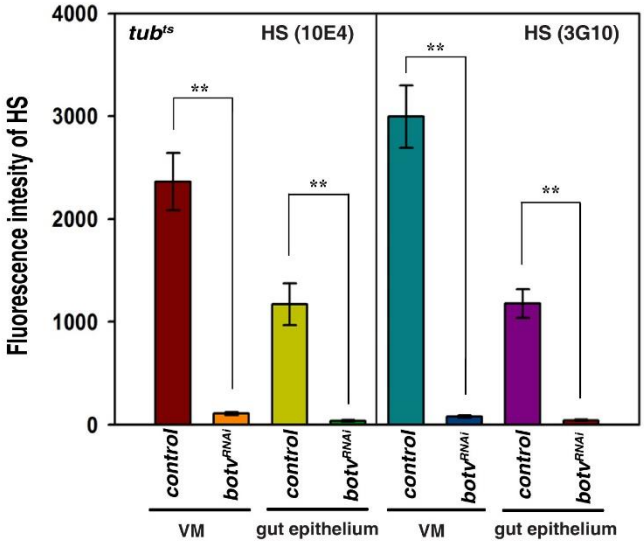

Fig. S4. HS is abrogated in *tub*^{ts}>*botv*^{RNAi} intestines. (A) Immunofluorescent staining for HS (by 10E4 and 3G10 in red) in the visceral muscles (VMs) and the gut epithelium of control intestines, respectively (white and yellow arrowheads, left panels). *botv* deletion abrogated HS staining (both by 10E4 and 3G10) in the VMs and the gut epithelium (white and yellow arrowheads, right panels). Split channel for HS (in black-white) was shown (yellow arrowheads). (B) Quantification of mean fluorescent intensity of HS (by10E4 and 3G10) in control and *tub*^{ts}>*botv*^{RNAi} intestines. $n \geqslant 4$. means ± SD is shown. $^{**}p < 0.01$. Blue indicates DAPI staining for DNA (except graphs). Scale bars: 10 μm.

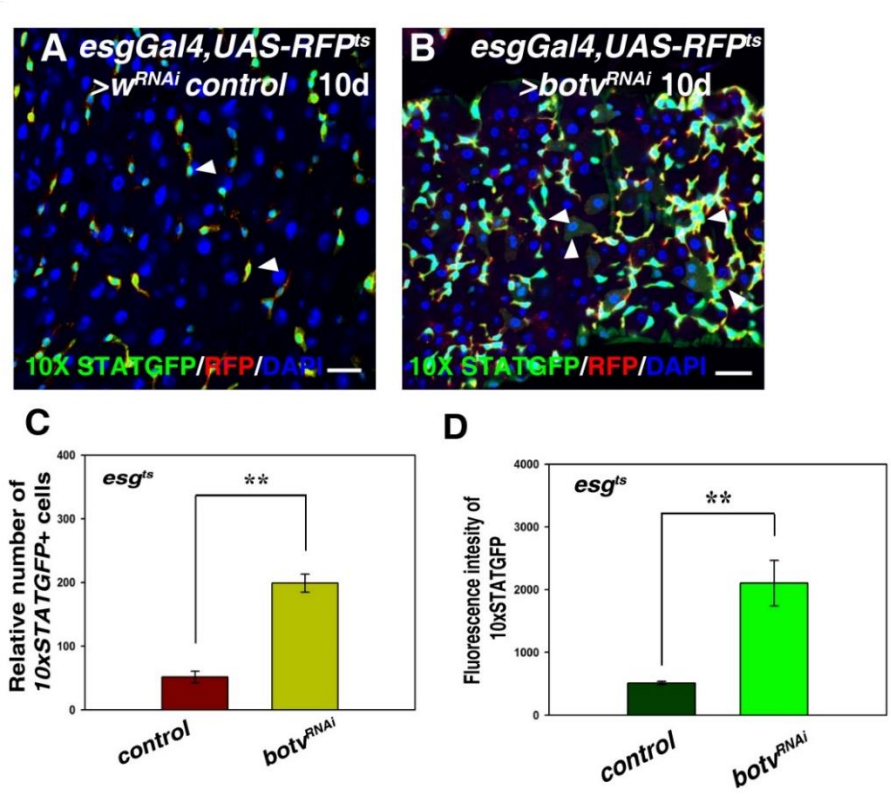

Fig. S5. JAK/STAT signaling is activated upon HS depletion in progenitors. (A) JAK/STAT signaling (by *10xSTATGFP*, green) in control intestines (*esgGal4^{ts}>RFP* to label progenitors in red) (white arrowheads). Note that *10xSTATGFP* is only activated in progenitor cells in the intestinal epithelium of control. (B) JAK/STAT signaling (by *10xSTAT-GFP*, green) is highly activated in *esg^{ts}>botv^{RNAi}* intestines (white arrowheads). (C) Quantification of the relative number of *10xSTATGFP^{+}* cells in control and *esg^{ts}>botv^{RNAi}* intestines. *n* = 10-15 testes. mean ± SD is shown. ***p*< 0.01. Please note that accurate quantification of the number of *10xSTATGFP^{+}* cells in *esg^{ts}>sfl^{RNAi}* and *esg^{ts}>botv^{RNAi}* intestines is not feasible as midgut homeostasis is lost in these intestines. (D) Quantification of fluorescence intensity of *10xSTATGFP^{+}* in control and *esg^{ts}>botv^{RNAi}* intestines. *n* = 10. mean ± SD is shown. ***p*< 0.01. Blue indicates DAPI staining for DNA. Scale bars: 20 μm.

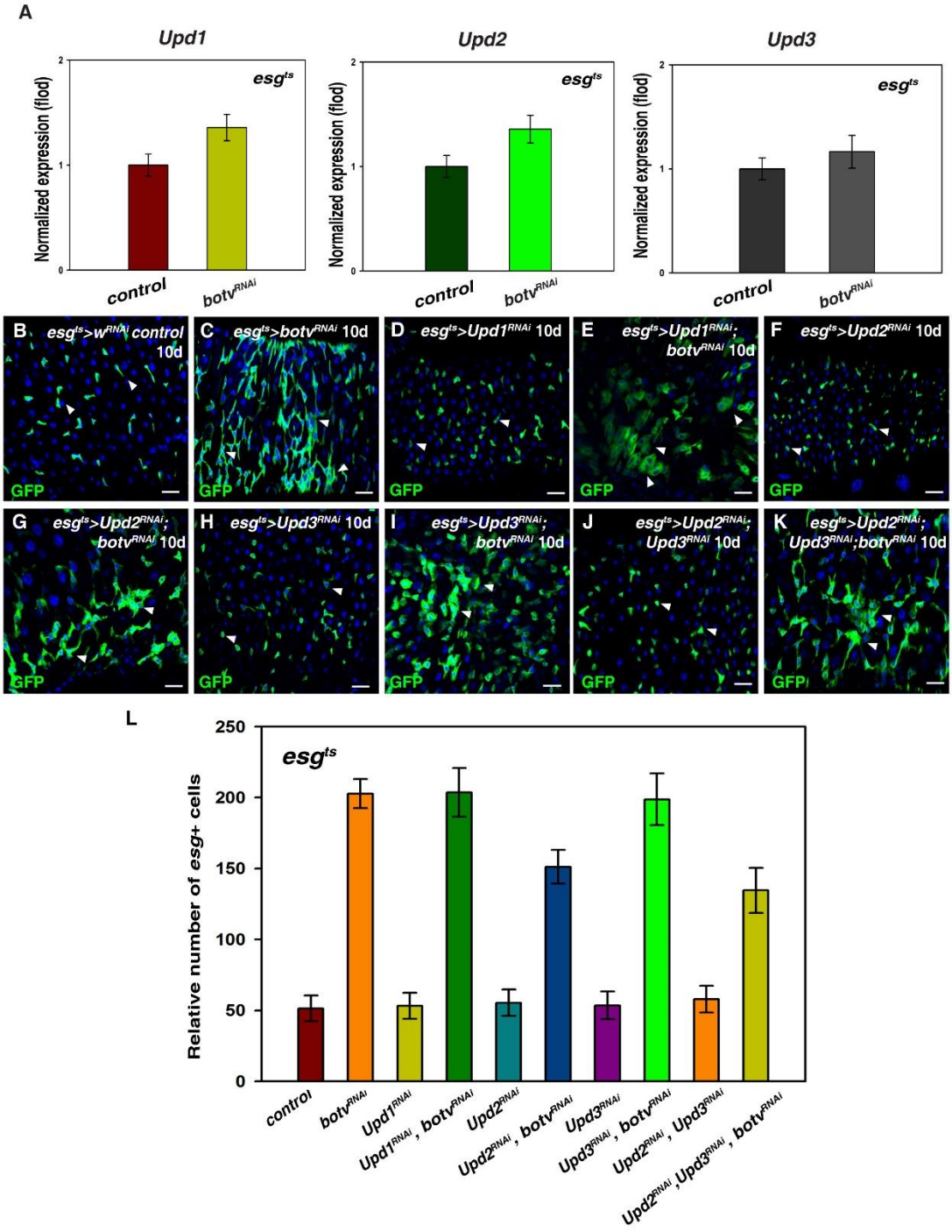

Fig. S6. Upds are unlikely produced in *HS-deficient* progenitors. (A) qRT-PCR quantification of *Drosophila* cytokines (*Upd1*, *Upd2*, and *Upd3*) mRNA expression from $esg^{ts}>botv^{RNAi}$ whole midguts at 29°C for 10 days. Ribosomal gene *RpL11* was used as normalization control. mean ± SD are shown. (B) esg^{+} cells (green) in control flies at 29°C for 10 days (white arrowheads). (C) The number of esg^{+} cells (green) is

dramatically increased in *esg*^{ts}>*botv*^{RNAi} flies at 29°C for 10 days (white arrowheads). (D) *esg*$^{+}$ cells (green) in *esg*^{ts}>*Upd1*^{RNAi} flies at 29°C for 10 days (white arrowheads). (E) No significant change in the number of *esg*$^{+}$ cells (green) is observed in *esg*^{ts}> *Upd1*^{RNAi}, *botv*^{RNAi} flies compared to those in *esg*^{ts}>*botv*^{RNAi} flies at 29°C for 10 days (white arrowheads). (F) *esg*$^{+}$ cells (green) in *esg*^{ts}>*Upd2*^{RNAi} flies at 29°C for 10 days (white arrowheads). (G) No significant change in the number of *esg*$^{+}$ cells (green) is observed in *esg*^{ts}> *Upd2*^{RNAi}, *botv*^{RNAi} flies compared to those in *esg*^{ts}>*botv*^{RNAi} flies at 29°C for 10 days (white arrowheads). (H) *esg*$^{+}$ cells (green) in *esg*^{ts}>*Upd3*^{RNAi} flies at 29°C for 10 days (white arrowheads). (I) No significant change in the number of *esg*$^{+}$ cells (green) is observed in *esg*^{ts}> *Upd3*^{RNAi}, *botv*^{RNAi} flies compared to those in *esg*^{ts}>*botv*^{RNAi} flies at 29°C for 10 days (white arrowheads). (J) *esg*$^{+}$ cells (green) in *esg*^{ts}>*Upd2*^{RNAi}, *Upd3*^{RNAi} flies at 29°C for 10 days (white arrowheads). (K) No significant change in the number of *esg*$^{+}$ cells (green) is observed in *esg*^{ts}> *Upd2*^{RNAi}, *Upd3*^{RNAi}, *botv*^{RNAi} flies compared to those in *esg*^{ts}>*botv*^{RNAi} flies at 29°C for 10 days (white arrowheads). (L) Quantification of the relative number of *esg*$^{+}$ cells in intestines with indicated phenotypes. *n* = 10-15 intestines. mean ± SD is shown. Blue indicates DAPI staining for DNA. Scale bars: 20 μm.

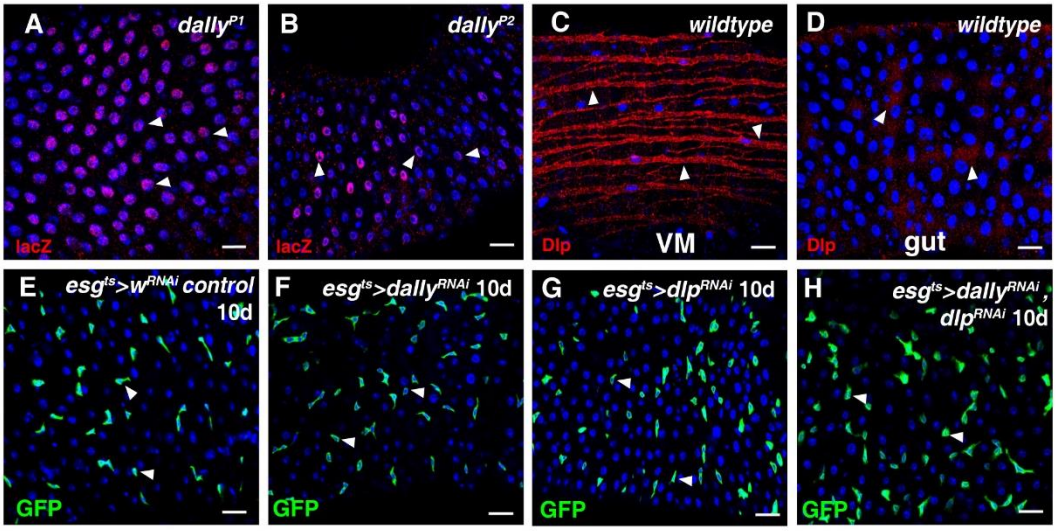

Fig. S7. HSPGs (except Per) are likely redundant for ISC proliferation. (A and B) Expression pattern of *dally* (by $dally^{P1}$ (A) and $dally^{P2}$ (B) in red) in intestines. *dally* (by *dally-lacZ*) is mainly expressed in ECs (white arrowheads). (C and D) Expression pattern of Dlp (red) in intestines. High levels of Dlp can be detected in the visceral muscles (VMs) and low levels in the intestinal epithelium (white arrowheads). (E) esg^+ cells (green) in control intestines at 29°C for 10 days (white arrowheads). (F) esg^+ cells (green) in $esg^{ts}>dally^{RNAi}$ intestines at 29°C for 10 days (white arrowheads). (G) esg^+ cells (green) in $esg^{ts}>dlp^{RNAi}$ intestines at 29°C for 10 days (white arrowheads). (H) esg^+ cells (green) in $esg^{ts}>dally^{RNAi}$, dlp^{RNAi} intestines at 29°C for 10 days (white arrowheads). GFP in green, blue indicates DAPI staining for DNA. Scale bars: 20 μm.

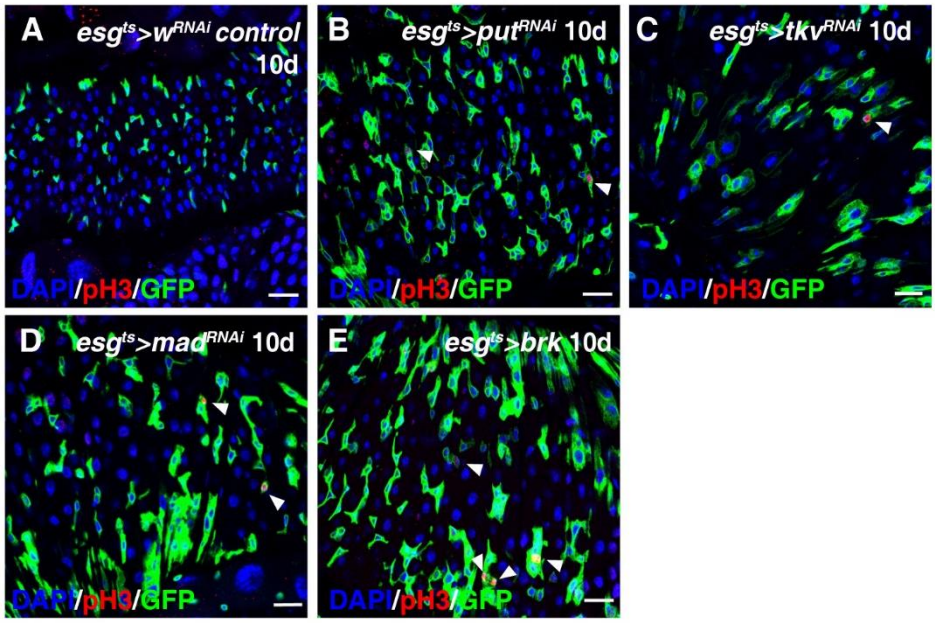

Fig. S8. ISC division is increased in the absence of Dpp signaling. (A) pH3 (red) in control intestines. (B) pH3 (red) in *esg*^{ts}>*put*^{RNAi} intestines (white arrowheads). (C) pH3 (red) in *esg*^{ts}>*tkv*^{RNAi} intestines (white arrowhead). (D) pH3 (red) in *esg*^{ts}>*mad*^{RNAi} intestines (white arrowheads). (E) pH3 (red) in *esg*^{ts}>*brk* intestines (white arrowheads). GFP in green, blue indicates DAPI staining for DNA. Scale bars: 20 μm. Please refer to Fig. 4G for quantification data.

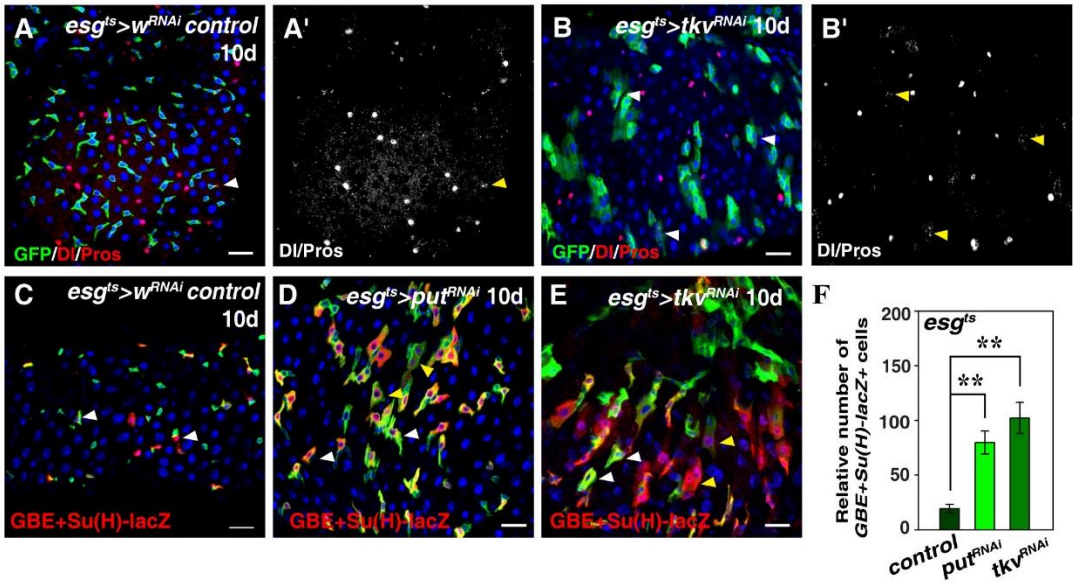

Fig. S9. Dpp signaling negatively regulates ISC proliferation and differentiation. (A) Dl and Pros (red) in control intestines at 29°C for 10 days (white arrowhead). Split channel for Dl and Pros (A', in black-white) in control intestines (yellow arrowhead). (B) Dl and Pros (red) in $esg^{ts}>tkv^{RNAi}$ intestines at 29°C for 10 days (white arrowheads). Split channel for Dl and Pros (B', in black-white) in $esg^{ts}>tkv^{RNAi}$ intestines (yellow arrowheads). (C) EBs (by *GBE+Su(H)-lacZ* in red) in control intestines at 29°C for 10 days (white arrowheads). (D) EBs (red) in $esg^{ts}>put^{RNAi}$ intestines at 29°C for 10 days (white arrowheads). Note that the size of the larger *GBE+Su(H)-lacZ*$^{+}$ cells is smaller compared to the size of the neighboring wildtype EC cells (polyploid *GBE+Su(H)-lacZ*$^{-}$ cells), indicating that Dpp signaling also affects EC maturation (yellow arrowheads). (E) EBs (red) in $esg^{ts}>tkv^{RNAi}$ intestines at 29°C for 10 days (white arrowheads). Note that the size of the larger *GBE+Su(H)-lacZ*$^{+}$ cells is smaller compared to the size of the neighboring wildtype EC cells (polyploid *GBE+Su(H)-lacZ*$^{-}$ cells), indicating that Dpp

signaling also affects EC maturation (yellow arrowheads). (F) Quantification of the relative number of *GBE+Su(H)-lacZ*$^{+}$ cells in control, *esg*^{ts}*>put*^{RNAi}, and *esg*^{ts}*>tkv*^{RNAi} intestines. n = 10-15 intestines. mean ± SD is shown. **p< 0.01. GFP in green, blue indicates DAPI staining for DNA. Scale bars: 20 μm.

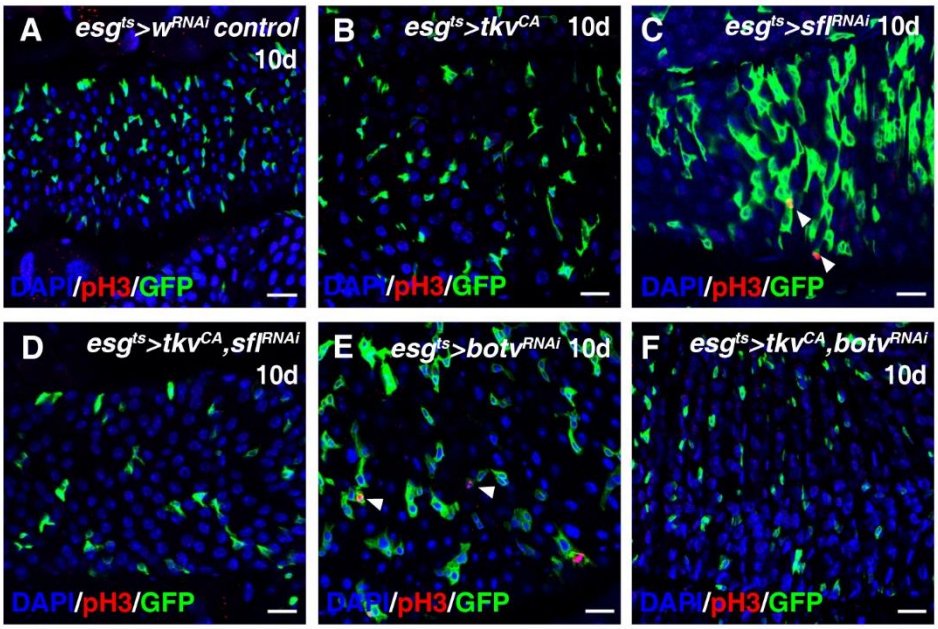

Fig. S10. Ectopic activation of Dpp signaling in progenitors completely rescued increased ISC proliferation in the absence of HS. (A) pH3 (red) in control intestines. (B) pH3 (red) in *esg*^{ts}>*tkv*^{CA} intestines. (C) pH3 (red) in *esg*^{ts}>*sfl*^{RNAi} intestines (white arrowheads). (D) pH3 (red) in *esg*^{ts}>*tkv*^{CA},*sfl*^{RNAi} intestines. (E) pH3 (red) in *esg*^{ts}>*botv*^{RNAi} intestines (white arrowheads). (F) pH3 (red) in *esg*^{ts}>*tkv*^{CA},*botv*^{RNAi} intestines. GFP in green, blue indicates DAPI staining for DNA. Scale bars: 20 μm. Please refer to Fig. 5H for quantification data.

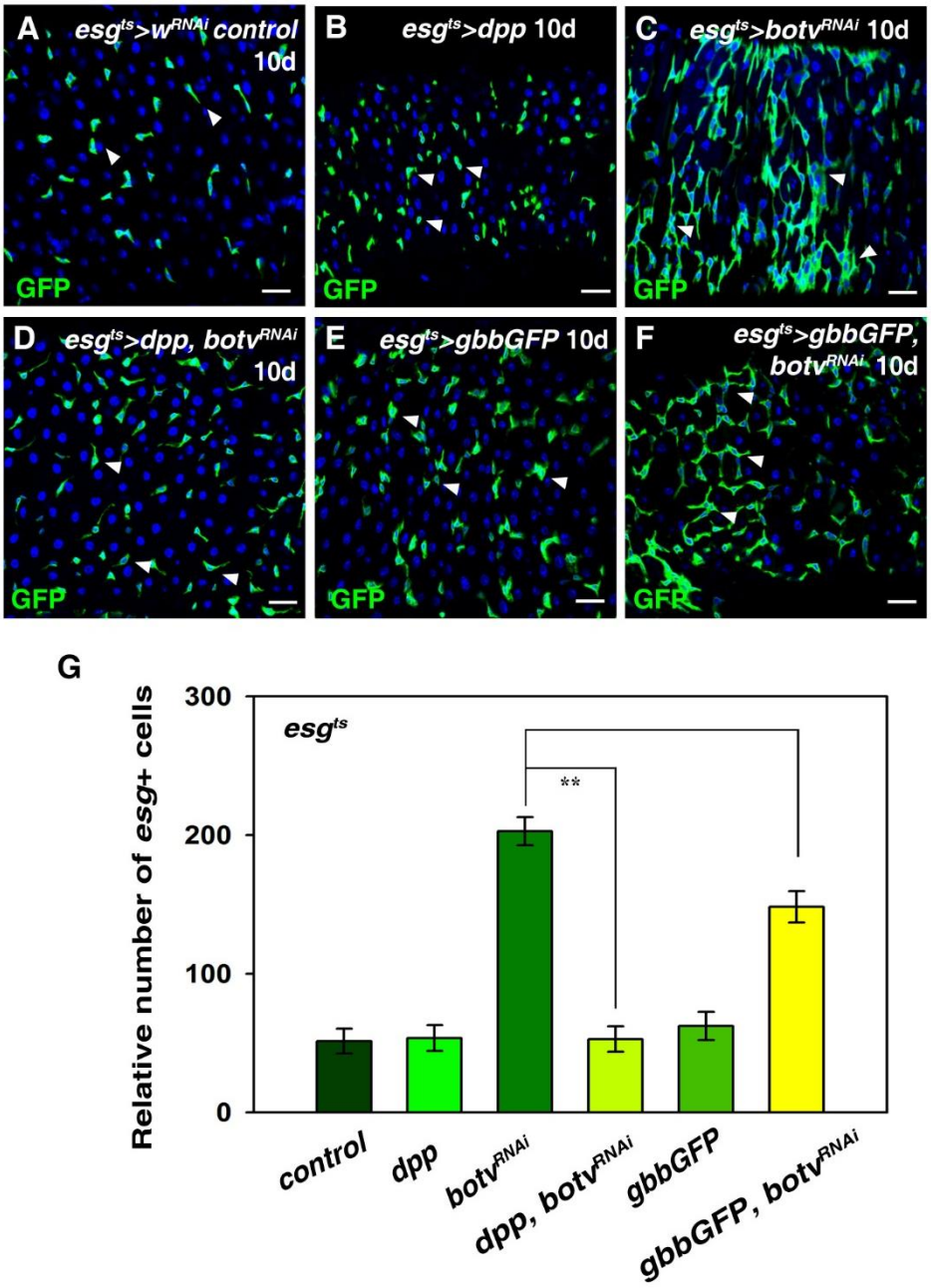

Fig. S11. Preference between Dpp and Gbb by HS.

(A) *esg*$^{+}$ cells (green) in control flies at 29°C for 10 days (white arrowheads). (B) *esg*$^{+}$ cells (green) in *esg*^{ts}*>dpp* flies at 29°C for 10 days (white arrowheads). (C) The number of *esg*$^{+}$ cells (green) is dramatically increased in *esg*^{ts}*>botv*^{RNAi} flies at 29°C for 10 days (white arrowheads). (D) The accumulation of *esg*+ cells in *esg*^{ts}*>botv*^{RNAi} flies is completely suppressed by co-expression of *UAS-dpp* at 29°C for 10 days (white

arrowheads). (E) *esg*$^{+}$ cells (green) in *esg*^{ts}*>gbbGFP* flies at 29°C for 10 days (white arrowheads). (F) The accumulation of *esg*+ cells in *esg*^{ts}*>botv*^{RNAi} flies is only partially suppressed by co-expression of *UAS-gbbGFP* at 29°C for 10 days (white arrowheads). (I) Quantification of the relative number of *esg*$^{+}$ cells in different genotypes indicated. mean ± SD is shown. *n* = 10-15 intestines. ***p*< 0.01. GFP in green, blue indicates DAPI staining for DNA. Scale bars: 20 μm.

Table S1. qRT-PCR primers used

RpL11-F: GGTCCGTTCGTTCGGTATTCGC

RpL11-R: GGATCGTACTTGATGCCCAGATCG

sfl-F: GGGATCGCCACGTTTCATG

sfl-R: CCGCAGATCCTTCAGTGCCC

sgl-F: GCGCTGGATATCTACGATCCG

sgl-R: GTAGGCTGGCTTCATCATCG

ttv-F: GGATGCCGTTCTGTCGCTGG

ttv-R: GTGGTAGAATGCCGCCCCAG

sotv-F: GACAACTATGTGCTACCCTTCG

sotv-R: AGTACTTGGAGAACAACCAC

botv-F: GCGTATGCAGGCGAAGGAAG

botv-R: GGTGAACTGCTCCCGGGGG

Upd1-F: GGTGATGGACCGCTGATCCCAG

Upd1-R: CCGCAGCCTAAACAGTAGCCAGG

Upd2-F: CAAGTCTTTAGCTTCACCGCACTTGTG

Upd2-R: CAAGGACGAGTTATCAAGCGCAAGC

Upd3-F: ATCACCACCAATGCGGACAAGC

Upd3-R: TGGCCAGGTCCCAGTGCAACT